MOLECULAR MECHANISMS CONNECTING GENOTYPE AND PHENOTYPE IN *Tbx1* DEFICIENCY

Julie De Mesmaeker

DEPARTMENT OF CARDIOVASCULAR MEDICINE

Submitted for the degree of

Doctor of Philosophy

EXETER COLLEGE
UNIVERSITY OF OXFORD
Michaelmas 2011

This thesis is dedicated to Claudio and Amélie with all my love

Contents

ABSTRACT

Background: The 22q11 deletion syndrome (22q11DS), also known as DiGeorge Syndrome, affects ~1/5000 live born children. Congenital heart defects (typically outflow tract and interrupted aortic arch) are present in 75% of individuals with 22q11DS and are the major cause of mortality. Other defects are cleft palate, thymus hypoplasia, inner ear defects and neuropsychiatric abnormalities. *Df(16)1* mice carry a ~1 Mb hemizygous deletion on mouse chromosome 16 in a region syntenic with 22q11 and phenocopies 22q11DS. TBX1 is a DNA-binding transcription factor located in this interval and is required for neural crest cell proliferation and migration and for cardiac development. *TBX1* point mutations have been identified in patients with DiGeorge syndrome. Thus *TBX1* is thought to be a major gene responsible for the cardiac phenotype in 22q11DS.

A key unresolved issue is the mechanism of reduced penetrance of cardiac malformations. One possibility is environmental variation during cardiogenesis. Supporting this idea, epidemiologic studies indicate that maternal obesity is associated with increased risk for cardiac defects, and in mice, a maternal high-fat diet interacts with embryonic *Cited2* genotype to enhance penetrance of left-right patterning and palate defects, and reduces thymus size irrespective of genotype. A second possibility is that variation in the TBX1 protein interaction network results in variable penetrance of the phenotype. Mutations in TBX1 or interacting partners could affect the structure of this protein interaction network.

Aim: The aim of this thesis is to characterize the molecular mechanism of *TBX1* function using biochemical and genetic approaches and to define the role of environmental variation on the DiGeorge phenotype.

Results *First part. Interaction of Df(16)1 with high-fat maternal diet.* To determine if a maternal high-fat diet affects the penetrance of cardiac and thymus malformations in the *Df1* deletion mouse model, wild-type and *Df1* heterozygous embryos from control and high-fat diet groups were analyzed. No significant difference in the penetrance or the severity of cardiac malformations between these groups was found. These results do not support the idea that change in the fat content of maternal diet affects phenotype in this model. Thus, it is possible that high-fat diet interacts specifically with left-right patterning rather than with the genetic control of pharyngeal arch development and neural crest cell migration and survival.

Second part. George, a novel ENU induced mutation in Tbx1. The *George* mutation, identified and mapped to Chr16 between rs4161352 and D16Mit112, results in fully penetrant cleft palate, cardiac malformations (VSD, IAA, CAT), absent cochlea and abnormal semicircular canals, and absent thymus resembling the human DiGeorge phenotype. *Tbx1* lies in this interval and sequencing identified a G > A point mutation in exon 3 which is predicted to cause a Arginine to Glutamine change at amino acid position 160. *George* fails to genetically complement a *Tbx1* null allele, confirming that it is causative and that George is functionally a null allele. RT-PCR showed that the George mutation affects splicing, resulting in a transcript lacking exon 3. This causes the loss of 34 amino acids within the TBX1 T-box domain, thus predicting that it affects DNA binding. Transactivation assays show that while the R160Q amino acid substitution significantly reduces the transactivation capacity of TBX1, surprisingly the loss of exon 3 does not affect this function. Analysis of endogenous TBX1 in developing embryos by Western blot showed that the protein expression is absent or significantly reduced. This finding suggests that the observed George phenotype is caused primarily by a loss of TBX1 protein expression.

Third part. Investigation of the protein interaction network surrounding TBX1. In order to get a better insight into the protein network surrounding TBX1, a TBX1 split renilla-luciferase protein complementation assay was set up which allowed to test the physical interaction between TBX1 and several putative interactors. It was found that GATA4, SMARCAD1, RBBP5 and PTDSR interact with wild-type TBX1 in HEK293T cells. The R160Q point mutation and the loss of exon 3 affect some of these interactions supporting the idea that variation in the protein interaction network may, at least in part, be responsible for the DGS phenotype.

CHAPTER 1

Background and Introduction

1.1 Heart Development – Overview

The formation of a complex organ such as the heart involves a sequence of finely controlled developmental events that implicate a huge number of genes whose expression is regulated in time and space. A first set of genes is involved in the regulation of the initial differentiation of mesodermal cells into cardiomyocytes (cardiac muscle cells). Cardiomyocytes originate from the lateral mesoderm and their differentiation is induced by the secretion of cardiogenic signals from the adjacent endoderm[1]. These signals, especially BMPs, activate the expression of cardiomyocyte-specific genes such as *Nkx2.5*, *Mef2c* and *Gata4* which in turn will activate an expression cascade of cardiac genes able to control cardiac morphogenesis and contractility[2-4]. As soon as the cardiomyocyte differentiation is complete, these cells converge ventrally in the embryo into a cardiac crescent before forming a linear heart tube. At this point it is already possible to distinguish two separate layers: the internal endocardium and the external myocardium. The linear heart tube is already divided into a series of virtual segments along the anterior-posterior axis and a separate set of genes is expressed in each of them[5]. This

will result in the rather independent morphogenesis of the different cardiac parts such as ventricle, atria, outflow tract etc.

The linear heart tube then undergoes a rightward looping which is determined by the assymetrical expression of a number of genes such as *Shh* and *Nodal*[5,6]. Once the heart looping is complete, the proliferation of cardiomyocytes within each chamber will allow the growth of the organ as well as its capability to support blood circulation. In order to separate the different heart chambers and allow only one-directional blood flow, the extracellular matrix located between the endocardial layer and the myocardial layer swells to form cardiac cushions. This process is regulated by factors secreted form the adjacent endo- and myocardium such as TGFß. The same kind of signals controls the transformation of some endocardial cells into mesenchymal cells before their migration into the cushions[7]. Once arrived at their final destination, these mesenchymal cells will differentiate into the fibrous tissue of the valves. The septation of the outflow tract into the aorta and the pulmonary trunk is accomplished by the migration of neural crest cells which originate from the neural folds. These cells also contribute significantly to the aortic and pulmonary arteries; however, the major part of the main aortic arch is derived from the pharyngeal arch arteries which develop independently from the heart[8].

Considering the complexity of the heart morphogenesis and the number of genes and factors involved, it becomes clear how a subtle perturbation of this process can cause severe cardiac malformations.

1.2 Congenital Heart Disease

Congenital Heart Disease (CHD) can be defined as a gross structural abnormality of the heart and intrathoracic great vessels resulting from abnormal heart development. The aberrations typically found in CHD include ventricular septal defects, outflow tract and valve defects, aortic/pulmonary arch defects and atrial septal defects. Each of these abnormalities can occur separately or in combinations with other defects. CHD is considered to be the most common birth defect in the UK affecting 1 in 145 live births (~ 4600 babies in the UK per year)[9-12]. It is associated with substantial morbidity and ~ 60% infant mortality if untreated, thus remaining the second cause of death in infancy after infectious diseases in the West. It is important to note that congenital heart disease is frequently associated with various neurological disorders which are considered to already be present in utero as a secondary effect of the heart defects. In addition to this, the multiple surgeries that are needed to correct many of the anatomical defects can be very debilitating and often result in a significantly reduced quality of life[13]. According to this, the WHO estimates that the global burden of CHD exceeds that of diabetes, hypertension, asthma and rheumatoid arthritis.

Mendelian and Chromosomal Syndromes such as Down's and DiGeorge Syndrome are believed to account for 20% of CHD cases. However, the majority of CHD (80%) is considered as "sporadic CHD" caused by rare de novo mutations[14,15]. The study of these cases has allowed the identification of numerous genes that are responsible for the occurrence of heart malformations. Most of these genes encode transcription factors that regulate the expression of specific proteins such as signalling molecules that are implicated in precise events during heart development, for example ventricular septation and outflow tract formation. The complex interaction between these transcription factors, in addition to their overlapping expression, allow for finely tuned regulation of the cardiac genes involved in different developmental processes[16].

Historically, the first single-gene mutation to be discovered in association with an inherited heart malformation disease, including ASD (Atrial Septal Defects), VSD (Ventricular Septal Defects) and conduction defects, was located in the T-box family gene, *TBX5*[17,18]. Today, this disease is referred to as Holt-Oram syndrome. Shortly after this discovery, mutations in *NKX2.5* were associated with severe heart defects such as ASD and TOF (Tetralogy of Fallot)[19,20]. *GATA4* was also shown to be associated with septation defects in patients carrying a mutation in this gene[21]. Of special interest for this research, *TBX1* has been identified as the single gene culprit for heart malformations associated with DiGeorge syndrome in patients who are not carrying the specific 22q11 microdeletion[22-24]. Single gene mutations in *Crkl*,

which is located within the critical DiGeorge deletion region, also result in complex cardiac defects in mice[25,26]. The transcription factor SALL4, which interacts with TBX5, is also part of this list of transcription factors linked to CHD and mutations in this protein have been pinpointed to be causing the heart defects in Okihiro syndrome[27-29]. Mutations in the T-box gene *TBX20* have been detected in families with VSDs, ASDs, ventricular growth and valve defects[30].

Further studies have made it clear that, in addition to the finding that haploinsufficiency of certain transcription factors might be enough to cause severe cardiac anomalies, defective interactions of these transcription factors with each other caused by a single mutation in either one of the interacting partners might underlie CHD. This was specifically shown by Garg V. *et al.*, in the case of GATA4-NKX2.5 and GATA4-TBX5 interactions[21] and by Hiroi, Y. *et al.* (2001)[31] in the case of NKX2.5 and TBX5 interaction where a point mutation in either of these genes increased the severity of the cardiac malformations. However, some mutations affecting these genes are only partially penetrant due to the existence of specific buffering mechanisms (i.e. duplicated gene, epigenetic and environmental mechanisms).

In addition to transcription factors, signalling molecules such as FGF8, NOTCH1, BMPs and WNTs are key players in the coordinated and harmonious development of the different cardiac structures and mutations in these genes have also been linked to cardiac malformations[32]. Moreover, little is known about the role played by chromatin modifying enzymes. It has previously been shown that the reduction of the chromatin remodelling complex BAF60C results in severe cardiac morphogenesis defects[33]. Histone modifying enzymes, such as SMYD1, are also thought to be crucial factors for proper heart development[34]. As discussed in chapter 1.5, mutations in these genes might affect cardiac gene expression dramatically through altering the interactions between transcription factors and their target promoter sequence.

In recent years, the influence of environmental factors on the occurrence of CHD has become more and more obvious. Maternal diabetes and obesity are both important risk factors for congenital heart disease[35] and are of particular interest when considering their increasing prevalence in western countries. It has been reported that diabetic mothers have a 3 fold, and obese mothers a 2 fold higher risk to have a child with congenital heart malformations[36,37]. Several studies have shown a clear link between maternal diabetes and severe cardiac malformation in the offspring, including laterality, looping and ventricular septal defects, transposition of the great arteries as well as outflow tract defects. To date, no precise pathogenic mechanism linking high glucose level to the heart defects has been found.

However, evidence points to the fact that the increased blood glucose level might affect the expression of some key regulatory cardiac genes leading to altered developmental pathways in the embryo[38]. Oxidative stress has also been shown to result from altered metabolic processes and the generation of free radicals might lead to cell damage in early development[39,40]. It has also been suggested that the effect of diabetes on development is mediated via altered epigenetic patterns[41].

Maternal illnesses such as rubella and influenza have been linked to birth defects especially when occurring at the very early stages of gestation. It has been reported that mothers affected by any febrile illness during the first trimester of pregnancy have a 2-fold higher risk of offspring with any cardiac malformation. The precise mechanism by which febrile illness causes embryonic heart defects is not known, but increased apoptosis is thought to play a major role. This is due to the implication of apoptosis in important cardiac developmental processes and its sensitivity to fever[42-44].

The effect of maternal alcohol consumption on cardiac development (fetal alcohol syndrome) has been documented by several studies and is thought to be caused by the effect of ethanol on the turgor of the primitive cardiac loop[45]. The use of teratogenic drugs such as antiviral drugs, certain antibiotics, folate antagonists and anti-inflammatory drugs has also been linked to an increased prevalence of heart defects in offspring[46-51]. CHD can therefore be considered a

complex genetic disease involving multiple genes, which in turn interact with each other as well as with environmental factors.

1.3 Maternal Obesity and Congenital Heart Malformations in the offspring

Obesity is one of today's major public Health problems especially in the industrialized/western countries. It is a fast expanding epidemic affecting more than 400 million people worldwide (WHO, 2005) and its prevalence is expected to rise to more than 700 million people by 2015 (WHO, 2005). In addition to causing serious health problems such as cardiovascular disease, diabetes and cancer, obesity is also associated with an increased risk of birth defects in infants from obese women. Several epidemiological studies have shown that obese mothers have an increased risk of offspring with neural tube defects[52-54], limb reduction anomalies[55], cleft palate[56] and cardiovascular malformations[36,57-59].

To date, the mechanism linking maternal obesity to birth defects is still unknown. However, a number of hypotheses have been put forward to explain this phenomenon. One possible explanation might be the presence of undiagnosed diabetes in association with hyperglycemia and increased insulin levels. As discussed in the previous section, diabetes is in fact a known risk factor for birth defects. Alternatively, the observed birth defects might result from

nutritional deficiencies linked to poor quality diets[60]. Moreover, obese women may have an increased requirement for certain nutrients such as essential vitamins. Finally, it has also been hypothesised that due to the increased difficulty during ultrasound scanning in obese women, some fetal malformation might not be detected, resulting in fewer terminations of pregnancy[61].

1.4 DiGeorge Syndrome and mouse model

DiGeorge Syndrome (22q11.2 deletion syndrome, DGS) is a complex developmental disorder that affects ~1/5000 children. DGS patients typically present thymus and parathyroid defects as well as craniofacial anomalies and psychiatric disorders[62]. Moreover, 75% of these individuals have congenital heart malformations including tetralogy of Fallot, ventricular septal defects, interrupted aortic arch, common arterial trunk and pulmonary stenosis, which represent the major cause of mortality[63]. In addition, several minor abnormalities have been reported in DGS patients such as genitourinary anomalies, scoliosis, short stature and hypocalcemia (http://www.vcfsef.org).

Whereas the earliest references to 22q11DS appeared in papers in the 1970s[64], the genetic causes underlying this disease have only become clear more than 20 years later with the important advances in genetics and molecular biology techniques, such as FISH and high

throughput sequencing[65-68]. Evidence was found that DGS resulted most commonly from a heterozygous 3 Mb (containing about 40 genes) or a nested 1.5 Mb deletion (containing about 30 genes) of chromosome 22q11[69]. The recurrence of deletions of uniform size is due to the presence of low copy repeat sequences flanking the 3Mb and the 1.5Mb deletion regions[65,66,68,70]. These observations suggested that one or more genes on human chromosome 22 were responsible for the observed DGS phenotype.

In order to elucidate the molecular basis of this syndrome and to identify candidate genes in the deleted region, several mouse models deleting a region of chromosome 16, syntenic with human chromosome 22, have been generated[71]. Lindsay *et al*. generated mice carrying a heterozygous deletion named *Df(16)1*, encompassing around 1 Mb and causing cardiovascular abnormalities characteristic of the human disease, including interrupted aortic arch, ventricular septal defects and outflow tract anomalies like pulmonary stenosis and overriding aorta[71]. These results suggest that critical genes for these defects are located in the *Df1* region (Figure 1).

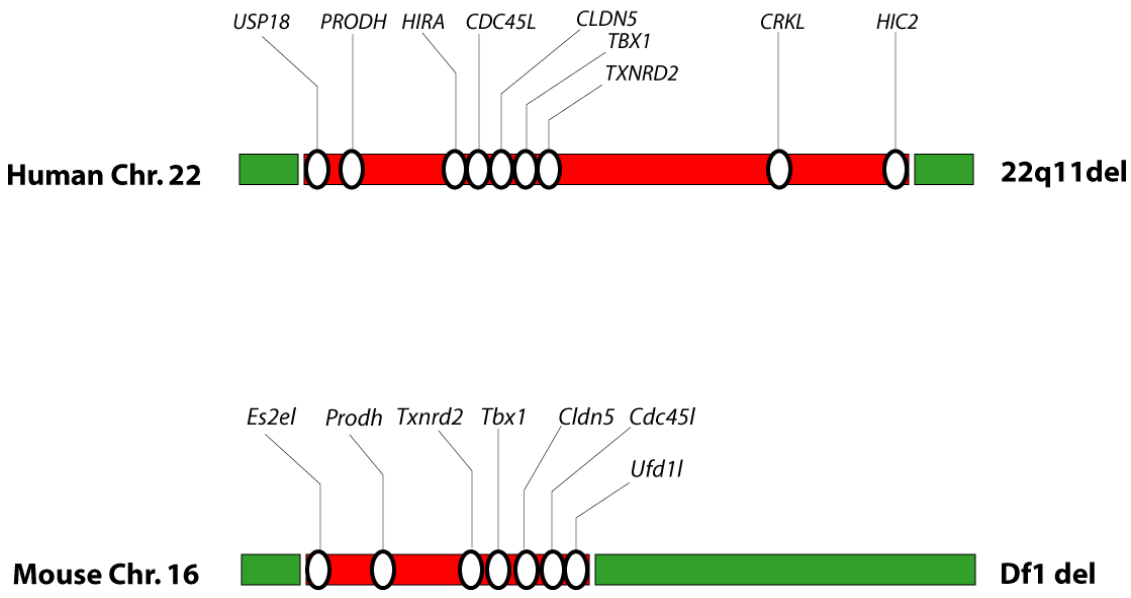

Figure 1. Schematic comparison between the human 22q11 deletion, and the mouse model deletion *Df1*. The red segments represent the deletions. Some of the main deleted genes are indicated in white circles. *TBX1/Tbx1*, *HIRA*, *TXRND2/Txrnd2* and *CRKL* are implicated in cardiac development.

The critical region was narrowed down to four genes, one of which was *Tbx1*, by further nested and overlapping deletions. Mice heterozygous for these genes were generated and *Tbx1*$^{+/-}$ mice were found to exhibit a more restricted phenotype than *Df1/+* mice (Table 1). *Tbx1*$^{+/-}$ mice exhibit aortic arch malformations, but only rarely do they have outflow tract defects. These only appear at a TBX1 dosage of < 20%[22,23,72,73].

Thus, whereas it is clear that *TBX1* plays a critical role in DGS, it is highly likely that other deleted genes contribute to the phenotype[69]. In fact, in addition to *TBX1*, the 22q11 deletion comprises other cardiac developmental genes such as *HIRA* [74], *CRKL* [26,75] and *TXNRD2*[76]. However, *TBX1* is the only gene for which mutations have been found in patients with the characteristic DGS phenotype who lack the chromosomal deletion[24,77,78].

	Human	Mouse	
	22q11del	Tbx1+/-	Df1/+
genetic architecture	heterozygous ~3Mb chromosomal deletion	Tbx1 knock-out	heterozygous ~1Mb chromosomal deletion
Heart phenotype	AoA and OFT defects	AoA defects	AoA and OFT defects
Penetrance of CHD	80%	28%	30%
thymus	hypoplastic	hypoplastic	hypoplastic
others	craniofacial anomalies, hearing impairement, psychiatric disorders	none	none

Table 1. Phenotypic comparison between the human 22q11 deletion, the mouse knock-out model *Tbx1*$^{+/-}$ and the *Df1/+* deletion model.

Tbx1 is a member of the T-box transcription factor family which is characterized by its conserved DNA-binding domain. *Tbx1* is necessary for the proper development of different tissues and organs such as heart, great arteries, thymus and parathyroid. All the DGS related anomalies are associated with the requirement of *Tbx1* for the development of the pharyngeal system[24,69]. Pharyngeal arches are temporary embryological structures that develop laterally to the head in a segmental fashion along the anterior-posterior axis. Initially, 6 pharyngeal arches develop and very early in development, the 5th arch resorbs while the 4th and 6th partially fuse together. Pharyngeal arches are composed of cells from all three germ layers and neural crest cells which originate from the neural tube and contribute to the pharyngeal arch mesenchyme.

In *Tbx1*$^{-/-}$ embryos, the first pharyngeal arch is abnormally patterned, the second is very hypoplastic and the third, fourth and sixth are not identifiable, whereas all the pharyngeal arches are hypoplastic in *Tbx1*$^{+/-}$ embryos[72]. Anomalies of neural-crest derived structures such as the cardiac outflow tract, aortic arch and thymus observed in *Tbx1* mutant mice are likely secondary to the effect of *Tbx1* on the development of the pharyngeal arches, where the proliferation and survival of neural crest cells during their migration through the region is adversely affected[72]. As *Tbx1* is not expressed in neural crest cells, the effects of *Tbx1* on these cells are thought to happen in a non-cell-autonomous manner. *Tbx1* is expressed in the second heart field, defined as a population of progenitor cells located in the pharyngeal mesoderm which contribute to the right ventricle and the outflow tract during heart morphogenesis. *Tbx1* positively modulates cell proliferation and inhibits differentiation and the effect of *Tbx1* on cell proliferation and survival is thought to be mediated by three separate mechanisms (Figure 2). The first mechanism is through the physical interaction between TBX1 and SMAD1[79]. This interaction leads to the sequestration of SMAD1 and eventually results in the inhibition of the BMP/SMAD1 signalling pathway which is involved in cell differentiation. Moreover, research has shown that BMP signalling also promotes myocardial differentiation through a different mechanism involving *Bmp2* and *Bmp4* regulated micro-RNAs that inhibit *Tbx1* transcription[80]. The second mechanism by which *Tbx1* promotes cell proliferation is through the transcriptional regulation of *Fgf8*[81]and *Fgf10*[82,83], two members of the fibroblast growth factor family. *Fgf8* and *Fgf10* have a mitogenic activity and interact genetically with *Tbx1*,

especially in the development of the outflow tract[83-86]. Recent findings indicate that not only is *Tbx1* regulating *Fgf8* expression, but its presence might be necessary for pharyngeal tissue response to *Fgf8*[87].

Finally, the migration of neural crest cells is thought to be controlled by *Tbx1* through its effect on expression of the transcription factor GBX2. Supporting this mechanism is the observation that the migrating streams of neural crest cells are completely disorganized in *Gbx2* mouse mutants lacking also a copy of *Tbx1*[88].

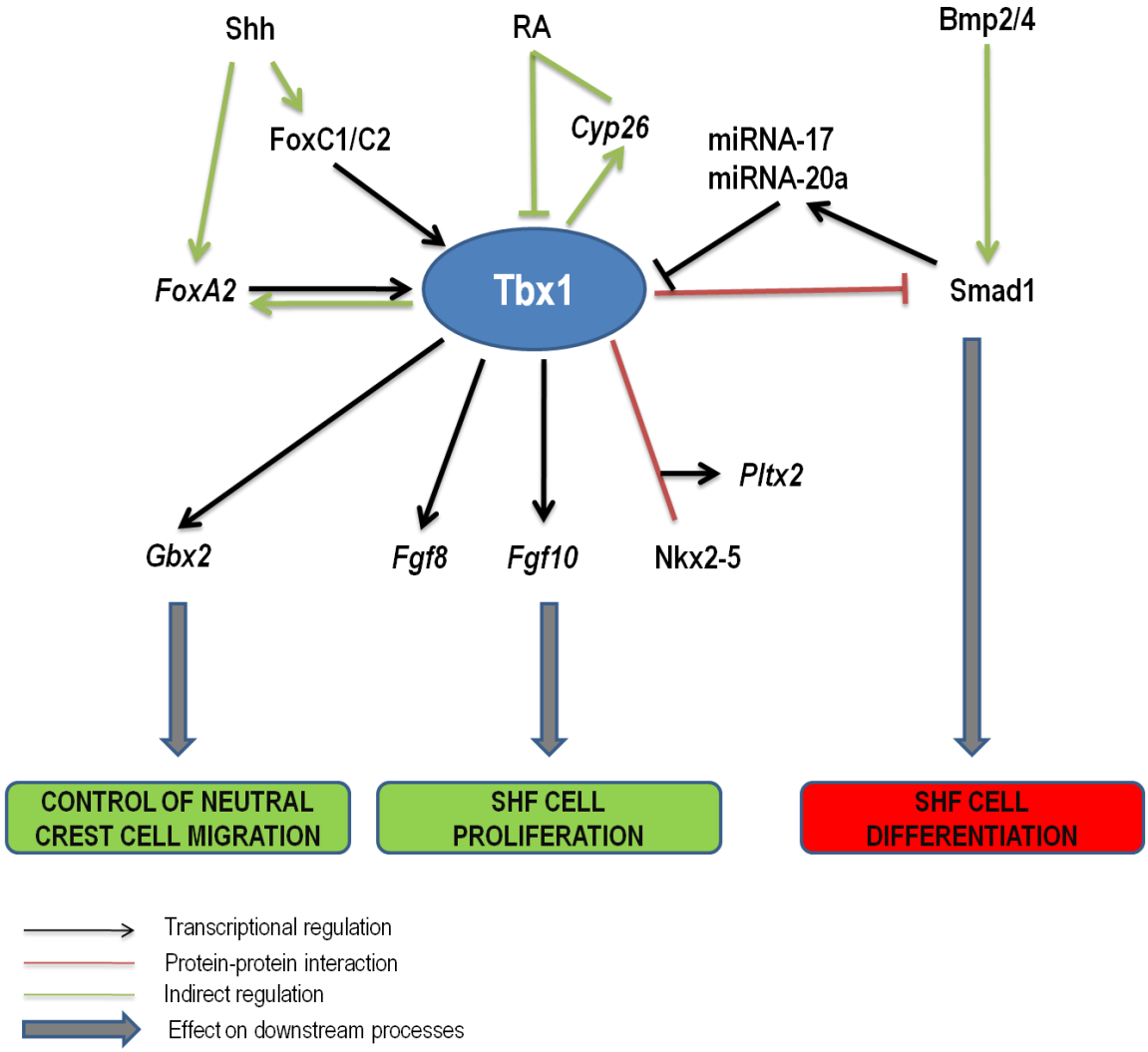

Figure 2. Summary of Tbx1 interactions in the regulation of SHF (Second Heart Field) cell proliferation and differentiation and neural crest cell migration (modified from Greulich, F., *et al.*, 2011)[89].

1.5 Mechanisms for phenotypic variation in DiGeorge Syndrome

Congenital heart defects are present in 75% of individuals with 22q11DS. The 22q11 deletion is inherited in an autosomal dominant fashion from a parent in approximately 6-28% of the cases[90,91]. However, parents transmitting this deletion only rarely (<5% cases) have cardiovascular malformations[90]. Moreover, a few monozygotic twin studies show discordance in the cardiovascular phenotype[92,93] . Likewise, this reduced penetrance is also observed in mouse models. For example, cardiovascular defects are present in 28% of *Tbx1*$^{+/-}$ and 30% of *Df1*/+ mice[25,71,73] (Table 1).

The variable penetrance observed in DiGeorge patients is likely to be due to a combined effect of genetic variation in the network around *TBX1* and environmental factors. The buffering of *TBX1* deficiency through compensation by other genes may account for the variable penetrance of heart defects. Some of these genes might be involved in the same genetic pathway, upstream or downstream of *TBX1* and therefore, any variation in these genes may affect the penetrance of DGS. Supporting this idea is the observation that *Tbx1* and *Vegf* genetically interact, and VEGF polymorphisms have been associated with a greater risk of cardiovascular defects in 22q11DS patients[94]. Recent findings report that *Chrd* also genetically interacts with *Tbx1* by modifying the craniofacial anomalies in *Tbx1* mutant mice[95]. *Pitx2* is also thought to be a genetic modifier of the cardiovascular defects seen in DGS as doubly heterozygous embryos show increased penetrance of DGS-related OFT defects. Moreover, it

has been shown that TBX1, together with NKX2.5, directly activates the *Pitx2c* enhancer. *Shh* is also considered to be a possible modifying locus for DGS. Supporting this hypothesis, *Shh*$^{-/-}$ embryos exhibit the same cardiovascular malformations that are found in DGS or *Tbx1*$^{-/-}$ embryos including aortic arch and outflow tract defects. It was also found that *Shh* might regulate *Tbx1* expression through *Foxa1*, *Foxc1* and *Foxc2*[96,97]. Interestingly, *Foxa1* is also a target of *Tbx1*, creating a positive feedback loop[81,96]. *Tbx1* and *Crkl*, which is also located in the 22q11 deletion region, show genetic interaction, as the compound heterozygote results in a striking increase in the penetrance and severity of the DiGeorge phenotype compared to the individual heterozygotes. Interestingly, *Crkl* promotes the intracellular response of FGF signalling by acting as an adaptor protein of the FGF-FGFR activated complex. It has also been suggested that *Tbx1* and *Crkl* regulate the expression of genes involved in retinoic acid metabolism, such as *Cyp26*, which has been shown to lead to a DiGeorge phenotype in mouse if perturbed[25,98,99]. Retinoic acid in its turn regulates the expression of *Tbx1* negatively[25,100,101] (please refer to figure 2 for summary). Retinoic acid is considered to be a potent teratogen as its deficiency, as well its excess, can cause heart defects in humans[102-104], and is a good example of how environmental factors could also be responsible for the variable penetrance of heart defects found in DGS patients. Maternal diabetes and obesity are both factors that could also potentially affect the DGS phenotype. This hypothesis is supported by the observation of a DGS-like phenotype in non-deleted offspring of mothers with preconceptional diabetes[105-108].

1.6 T-box family

The T-box gene family comprises 17 members in humans and homologues have been identified in the genomes of many other organisms[89]. Phylogenetic analysis and sequence alignment of the T-box sequences revealed that the T-box family has developed through gene duplications and cluster dispersion originating from a single common "ancestral gene"[109]. The T-box genes are organised in five subfamilies and all family members share some common features and the most defining one is their conserved DNA binding domain (T-box), which indicates a common function as transcription factors[110]. However, the T-box proteins differ dramatically in their ability to bind to one half (T half site) of a palindromic DNA target sequence (T-site) which might result in a differential modulation of the target gene expression. For example, in vitro experiments have shown that TBX1 binds to a T site as a dimer whereas a monomer of TBX2 was able to bind to the same T-site[111].

Secondly, expression studies have shown that the more closely related members such as *Tbx2*, *Tbx3*, *Tbx4* and *Tbx5* have overlapping expression patterns differing only by subtle spatial and temporal variations. Therefore, individual T-box family members may have unique as well as shared target genes[112].

A third feature shared between the T-box family members is their major involvement in embryonic development and many of them are crucial for proper heart morphogenesis. Of particular interest to this thesis is the role of *Tbx1* in the development of the pharyngeal arches where it positively modulates cell proliferation, inhibits cell differentiation and affects neural crest cell migration. Further examples are *Tbx5* and *Tbx20* which are involved in the cardiac chamber formation by acting as transcription regulators of genes controlling cardiomyocite differentiation[31,113]. *Tbx2* and *Tbx3* on the other hand act as local repressors of these myocardial differentiation pathways in order to allow valve formation[89,114]. All of the known mutations in T-box genes result in human developmental syndromes and play a significant role in inherited human disorders which makes the study of this gene family exceptionally relevant to medical sciences[115]. Of central interest for this thesis is *TBX1*, mutation of which can cause DiGeorge Syndrome characterised by the malformation of pharyngeal arch derived structures such as heart, thymus, palate and ear. Ulnar-mammary Syndrome is caused by mutations in *TBX3* and affects primarily the proper development of the limbs. Mutations in *TBX5* have been linked to Holt-Oram syndrome characterized by both cardiac and skeletal abnormalities. Finally, it has been shown, that the rather common cleft palate defect can be caused by mutations in *TBX22*. An important range of mutations have been found in these T-box genes and the most common ones generate null alleles that result in haploinsufficiency in human disease. Several missense mutations have also been identified which might affect the interaction of these T-box proteins with other cofactors[115].

For further information regarding the T-box gene family and its fundamental implication in vertebrate development, please refer to the excellent review by Naiche, L.A., *et al.*, (2005)[116]

1.7 Regulation of the genes involved in cardiac development

As discussed in a previous section, heart development is a complex process involving a large number of genes whose expression needs to be precisely regulated in order to assure proper morphogenesis of the organ. The transcriptional regulation of these genes depends on a large array of transcription factors and the interaction between these transcription factors represents an additional level of fine-tuned expression control. The primary function of transcription factor is to bind to the target promoter sequence and activate transcription by recruiting key cofactors and the transcription machinery. However, as the function of transcription factors is closely linked to the status of the chromatin at particular targets, the interaction between transcription factors and chromatin remodelling, as well as histone modification factors, can be considered as an additional level of spatial and temporal regulation of gene expression[117]. DNA transcription depends on whether the chromatin is open (euchromatin) or closed (heterochromatin). Euchromatin refers to a state in which the chromatin is loosely arranged around the histone which allows transcription factors to bind their target sequence and activate transcription whereas heterochromatin is tightly condensed and inaccessible for transcription factors resulting in transcription inhibition[118,119]. The establishment of one of these chromatin states is regulated through two distinct mechanisms. The first mechanism involves ATP-dependent remodelling protein complexes that use ATP hydrolysis as an energy source for altering the chromatin state[120]. Actions involving histone tail modification complexes, such as methylation, acetylation, ubiquitination and phosphorylation, represent the second mechanism

that affects the chromatin structure[117]. Finally, the last level of gene transcription regulation involves another epigenetic mechanism which is DNA methylation. DNA methylation occurs on CG-rich islands located in the gene promoters which results in transcription repression by shielding the promoter off transcription factors[121]. For a review see van Weerd *et al*., 2011[117].

Of particular interest in relation to the work presented in this thesis, recent studies have demonstrated that the interactions between BAF chromatin remodelling complexes and transcription factors such as NKX2.5, GATA4 and TBX5 play an essential role in the control of specific gene expression cascades during heart development[122]. Whereas the specific role of histone modifying methylases and demethylases in heart development is not yet known, a study focussed mainly on T-cells showed that two T-box proteins, namely T-BET and TBX5, interacted physically with and were able to recruit the histone demethylase JMJD3 and the histone methyltransferase RBBP5[123]. These results suggest that some T-box proteins are able to recruit multiple histone modifying enzymes that collaborate to render a target sequence ready for transcription activation. These observations indicate that T-box transcription factors might have a fundamental role in modifying and regulating epigenetic states of the DNA during development [124,125]. Supporting this idea, Miller *et al*., showed that mutations disrupting these interactions were found in several genetic disease patients[123].

1.8 ENU mutagenesis

One way to understand how genes are involved in developmental processes is to modify or delete specific genes and then assess how this affects embryogenesis. However, in the situation where the implicated genes are not known a priori, the use of Ethylnitrosourea (ENU) induced mutagenesis is a very powerful and efficient alternative to dissect the mechanisms through which biological processes occur[126].

ENU introduces point mutations by transferring its ethyl group to oxygen or nitrogen radicals of DNA which results in the alkylation of nucleic acids and then mispairing and basepair substitutions. The most common mutations induced by ENU are A/T to T/A transversions and A/T to G/C transitions which result in 64% missense mutations, 10% nonsense mutations and 26% splicing mutations when translated into a protein product[127].

ENU targets premeiotic spermatogonial stem cells and the frequency of ENU induced mutations is around 1 nucleotide change in every 1MB of genomic DNA, corresponding to roughly 1 loss of function mutation per gene in every 700 male gametes[128].

Depending on whether dominant or recessive mutations are of interest, the mutagenized males are crossed following a specific pattern and their progeny is phenotyped. Whereas only one cross between the mutagenized male and wild-type females is needed for a dominant screen, the crossing strategy for a recessive screen requires more generations in order to obtain homozygous mutant offspring (Figure 3).

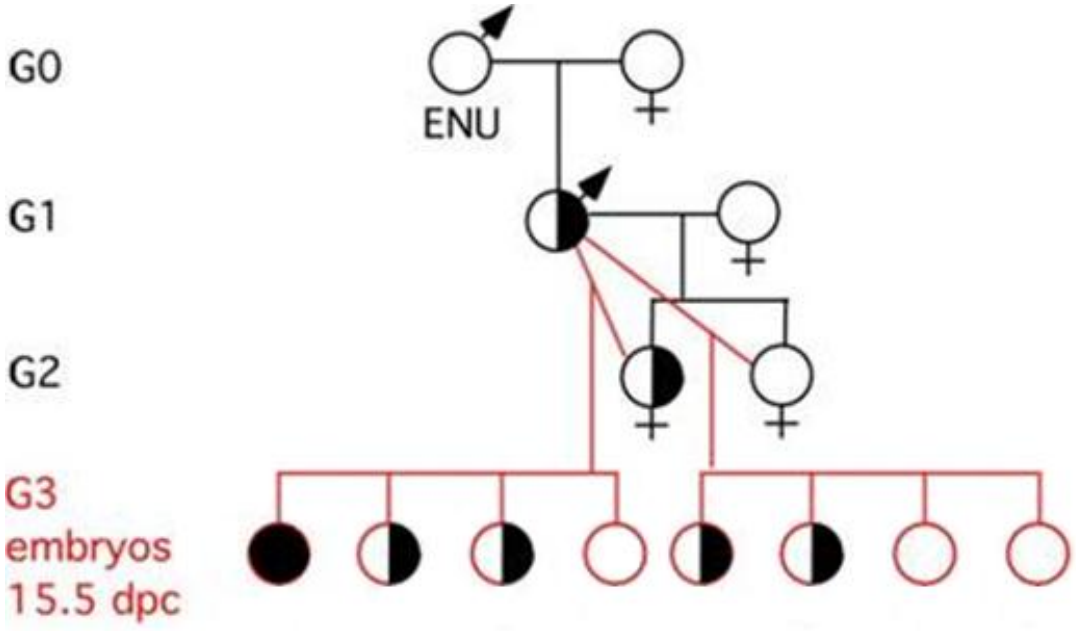

Figure 3 Mouse crossing strategy for recessive ENU screen. The mutagenized male is crossed with wild-type females (G0). The male offspring (G1) generated from the cross are crossed to wild-type females. The female offspring (G2) generated from this cross are then crossed to their father in order to obtain homozygous mutant embryos (G3) (Figure kindly provided by Dorota Szumska).

The advantage of screening recessive mutations instead of dominant ones is that the identification and the maintenance of the mutation of interest is much easier as dominant mutations causing heart malformations very often result in foetal or perinatal death. Following their identification, the segregation of the phenotype relative to molecular polymorphisms is assessed using a SNP-based PCR and sequencing approach.

As ENU is a point mutagen it can produce different types of alleles, for example loss of function, hypomorphs, antimorphs, neomorphs and even gain of function mutations.

Therefore, ENU mutagenesis is a very useful technique to uncover unknown functions of specific proteins. Other chemicals that are sometimes used as germline mutagens are chlorambucyl or radiation, which are used to obtain large deletions or inversions rather than point mutations[129].

1.9 Principal issues addressed in this thesis

The aim of this thesis is to investigate the molecular mechanisms connecting genotype to phenotype in *Tbx1* deficiency. The first part of this work concentrates on defining the role of environmental variation, specifically maternal high fat diet, on the severity and the penetrance of the DiGeorge phenotype in a mouse model. This will increase our knowledge on the role of gene-environment interaction in congenital heart disease.

The second part of this thesis focuses on the characterization of a *Tbx1* ENU point mutant, using a biochemical and genetic approach. This may shed some light on the molecular mechanism of *Tbx1* function.

And finally, the third part of this project is dedicated to getting a better understanding of the protein interaction network surrounding TBX1 and how perturbation in this network may result in variable penetrance and severity of the phenotype. This question was addressed using recently developed cell-based assays.

Taken together, the work presented in this thesis provides important clues to get a better understanding of the mechanisms underlying the variable penetrance associated with DiGeorge Syndrome. As a result, this might contribute to furthering our knowledge needed to develop preventive therapeutic strategies for Congenital Heart Disease.

CHAPTER 2

Materials and Methods

2 Introduction

This chapter is divided into three sections. The methods used to study the effect of maternal preconceptional high fat diet on the severity and penetrance of a DiGeorge mouse model are described in section 2.1. Section 2.2 details the methods used for the characterisation of the George ENU mutant. The methods used for the investigation of the protein interaction network surrounding TBX1 as well as the effect of the George mutation on these physical interactions are described in section 2.3.

2.1 High fat diet study

2.1.1 Mice:

All mutant mouse lines used were on a C57BL/6 background. *Df1/+*[130] and *Tbx1*$^{+/-}$ (*Tbx1*^{tm1Bld})[22] mice were kind gifts from Professor P. Scambler. *Tbx1*$^{+/Geo}$ mice were created through ENU mutagenesis. Mice and embryos were genotyped using DNA extracted from ear biopsies or forelimbs respectively. Analysis for *Df1/+* and *Tbx1*$^{+/-}$ genotyping were performed by PCR and the primers used are described in Lindsay *et al.* (2001)[22]:

The primers used for *Df1/+* genotyping were:

uftar2-f: 5'-tctttgtcagcagttcccttt-'3 and
ufdtar2-r: 5'-tgggcaattgtttaatcttcc-'3.
A third primer (*ufdwt3*: 5'-cagagttctgacttctgcacactaa-3') was used in multiplex (P. Scambler, personal communication);

The primers used for *Tbx1*$^{+/-}$ genotyping were:

tbxtar2-f: 5'-cagagaagggtcgcctacat-'3 and
tbxtar2-r: 5'-tcgactagagcttgcggaac-'3.

Tbx1$^{+/Geo}$ genotyping was performed by PCR followed by MspI restriction digest. The primers used were as follows:

gtTbx1_ex3F: 5'-tggagagtgttcctgtactc-3' and
gtTbx1_ex3R: 5'-actggatttggcgtcactag-3'.

2.1.2 Diet

Custom formulated control and high-fat diets where obtained from Special Diet Services, Witham, Essex, UK. The main difference between the diets was the energy source which is starch in the control diet versus fat and sugar in the high-fat diet. More precisely, the proportion of nutrients (%) in control versus high-fat diet is: fat 5.4/40; protein 20.3/20.3; ash 3.5/3.5; fibre 3.5/3.5; nitrogen-free extract (NFE) 62/28; sugar 34/27; starch 26/0. Trace minerals and vitamins were identical between the two diets apart from total vitamin D and E, which were higher in the high-fat diet as they are present in animal fat (Table 2)

Constituents	Control Diet	High fat Diet
Fat (%)	5	40
Protein (%)	20	20
Fibre (%)	4	4
Sugar (%)	34	27
Starch (%)	26	0
Vit A (iu/kg)	4000	4000
Vit E (iu/kg)	85	96
Vit B1 (mg/kg)	6	6
Vit B2 (mg/kg)	5	5
Vit B6 (mg/kg)	7	7
Vit B12 (ug/kg)	25	25
Folic Acid (mg/kg)	2	2
Nicotinic Acid (mg/kg)	30	30
Choline (mg/kg)	1081	1081
Biotin (ug/kg)	200	200

Table 2. Dietary constituents of control diet and intervention high-fat diet[131].

2.1.3 Diet induced obesity in mice

Six week old C57BL6/J wild-type females were obtained from Harlan Laboratories (Bicester, UK). They were randomly assigned to specially formulated control or high-fat diet, which were provided *ad libitum*. The mice were weighted at baseline and after 8 weeks on the diet. At the same time points, 6-hour fasting blood samples were taken for measuring insulin and

glucose levels. The blood samples were collected through a superficial vein under local anaesthesia.

2.1.4 Mating and embryo harvest

After 8 weeks on their respective diets, the 14 week old female mice were mated with *Df1/+* males and the diet continued through pregnancy. For studies of embryo development, the pregnant females were killed via cervical dislocation and the embryos were harvested at 15.5 dpc. One forelimb was used for genotyping by allele-specific PCR.

2.1.5 Embryo phenotype analysis

To detect malformations, the embryos were analysed by magnetic resonance imaging (MRI). Briefly, the embryos were fixed in 4% paraformaldehyde + 2mM Gd-DTPA (an MRI contrast agent). The embryos were then embedded in 8 layers of 4 embryos each in 1% agarose containing 2mM Gd-DTPA and analysed using the 11 Tesla magnet available in our department. The 3D MRI dataset obtained was reconstructed into 2048 axial TIFF slices and stored on DVDs. Images were analysed using Amira 5.2 software in transverse, coronal and

sagital axes. Thymus volumes were measured by segmentation analysis using the same software and all measurements were corrected for embryo weight.

2.2 Characterisation of *George*

2.2.1 ENU genome wide recessive screen for cardiac genes

Dr. Dorota Szumska identified the *George* allele in a genome wide recessive screen for cardiac genes as part of an ENU mutagenesis project. ENU mutagenised C56BL6/J males were crossed to wild-type C3H females. In order to bring any unique point mutation carried by a G1 animal to homozygosity, the G2 daugters were backcrosssed to their G1 father. The G3 offsprings were harvested at 15.5 dpc and screened for heart defects using MRI (Figure2). Once identified, the *George* line was mapped to a chromosomal region by SNP genotyping and the region was further narrowed by outcrossing. In order to identify the molecular lesion, PCR products of all exons and splice junctions of the most likely candidate gene, *Tbx1*, were sequenced.

2.2.2 Complementation test

Tbx1$^{+/Geo}$ mice were crossed to *Tbx1*$^{+/-}$ mice to obtain *Tbx1*$^{-/Geo}$ embryos. All embryos resulting from the cross were harvested at 15.5dpc and analysed by MRI in order to detect structural malformations.

2.2.3 RT-PCR

RT-PCRs were carried out on isolated mRNA extracted from pharyngeal arches and hearts of 10.5 dpc *Tbx*$^{+/+}$, *Tbx1*$^{+/Geo}$ and *Tbx1*$^{Geo/Geo}$ embryos. RNA was extracted using a Qiagen RNeasy Mini kit as per manufacturer's instructions. Whole mRNA RT was performed using QuantiTect Reverse Transcription Kit from Qiagen and 2 PCR exon spanning 21nt long primers were used. The primers were located in exon 2 and in exon 5:

ex2RT-f: 5'-gtgagcgtgcagctggagatg-'3
ex5RT-r: 5'-taggcagtgactgcagtgaag-'3.

The PCR products were purified using PCR purification kit from Qiagen and sequenced.

2.2.4 Cell culture

All the cell-based experiments were performed in HEK293T cells cultured in Dulbecco's modified Eagle's medium (DMEM; sigma) containing 10% fetal calf serum (sigma), 1% penicillin/streptomycin (invitrogen) and 4mM L-Glutamine (invitrogen). The cells were incubated at 37 C in a humidified atmosphere with 5% CO2.

2.2.5 Protein extraction from cells

HEK293T cells were cultured in 6 well-plates until 60% confluent and 1ng of plasmid was then transfected with Fugene HD (Invitrogen) following the manufacturer's protocol. After 24h incubation at 37 C the cells were washed once with PBS and scraped from the plates after adding 380ul SDS buffer (0.125M Tris pH 6.8, 4% SDS, 20% v/v glycerol, 5% BME and a few grains of Bromphenol Blue) was added to the cell lysate sample before use.

2.2.6 Protein extraction from tissue

After dissection, 5 10.5dpc pharyngeal arches of each genotype ($Tbx1^{+/+}$, $Tbx1^{+/Geo}$, $Tbx1^{Geo/Geo}$ and $Tbx1^{-/-}$) were pooled. The pharyngeal arches were lysed at RT in 1ml Lysis buffer (8M urea in Phosphate Buffer; 0.5% SDS and Laemmli) containing cOmplete, EDTA-

free protease inhibitor (Roche) and Laemmli buffer. The lysate was then centrifuged for 5min at 13000rpm. After centrifugation the supernatant was incubated for 30min on ice. Total protein quantification was performed using the BCA kit (Pierce) following the manufacturer's instructions.

2.2.7 Western Blot

For western blotting, 2x Laemmli was added to the lysates. Samples were then boiled for 5min and incubated on ice for an additional 5min. The proteins were separated by gel electrophoresis on a 10% polyacrylamide gel under denaturing conditions. Immunoblotting was performed using a goat anti-mouse TBX1 primary antibody (Abcam) and an IgG rabbit anti goat secondary antibody (Pierce).

2.2.8 Plasmid constructs

The CMV-Tbx1wt plasmid was kindly provided by A. Rauch. The CMV-Tbx1 R160Q and CMV-Tbx1 Ex3del plasmids were obtained by PCR based site-directed mutagenesis using the CMV-Tbx1wt plasmid as a template. For the CMV-Tbx1R160Q construct, the primer sequences were:

Product A;

Tbx1fwd: 5'-ttacgctagcatgcacttcag -3' and

Mutrev: 5'-ggcgtactggtagcgcttatc-3'

Product B:

Mutfwd: 5'- aagcgctaccagtacgccttc-3' and

Tbx1rev: 5'-gcactagttatctggggcaat-3'.

For the CMV-Tbx1 Ex3del construct, the primer sequences were:

Product A:

Tbx1fwd: 5'-ttacgctagcatgcacttcag -3' and

Ex3delrev: 5'-ctgtggaaggcgtacctgccggccttggtgacgatcatct-3'

Product B:

Ex3delfwd: 5'-caccaaggccggcaggtacgccttccacagctcctcctgg-3' and

Tbx1rev: 5'-gcactagttatctggggcaat-3'.

For each of the constructs, the PCR products A and B were annealed and elongated using the *Tbx1fwd* and *Tbx1rev* primers (Product C). For each of the constructs, the PCR product C was cloned into pGemT-Easy. The sequence of CMV-Tbx1wt was then replaced by the mutated sequence (R160Q or Ex3del).

2.2.9 Cell localization

HEK293T cells were grown on glass slides in 6-well plates until 30% confluent. 100ng Tbx1-mcherry constructs were transfected using FugeneHD (Promega) following the manufacturer's instructions. The cells were incubated at 37 degrees for 24h. The cells were then washed with PBS, fixed in 2% PFA for 10min at RT, then permeabilised for 10min at RT in PBT (PBS + 0.1% Triton) and incubated for 10 min at RT in PBS containing 10% DAPI before being mounted. The cells were analysed using Confocal imaging using a Zeiss 510 Metahead Laserscanning Confocal Microscope.

2.3 TBX1 Protein Interaction Network

2.3.1 Plasmid constructs

The plasmids used for the protein interaction assays were obtained using the Gateway cloning system (Invitrogen) following the manufacturer's instructions. The pENTR plasmids for *SMAD1, SMARCAD1* and *Ptdsr* were kindly provided by Prof A. Baldini, Dr. R. Kelly and Dr. Jens Bose respectively. The pENTR plasmids for *Gata4*, *NKX2.5* and *RBBP5* were constructed using inserts obtained through PCR using the following primers:

Gata4-attbfwd: 5'-aaaaagcaggctccaccatgtaccaaagcctggcc-3' and
Gata4attbrev: 5'-agaaagctgggtccgcggtgattatgtcccc-3';

Nkx2.5attbfwd: 5'-aaaaagcaggctccaccatgttccccagccctgcg-3' and
Nkx2.5attbrev: 5'- agaaagctgggtcccaggctcggatgccgtg-3';

Rbbp5attbfwd: 5'- aaaaagcaggctccaccatgaacctcgagttgctg-3' and
Rbbp5attbrev: 5'-agaaagctgggtctaacagttctgagattgc-3'.

The PCR products were then ligated into pGemT-easy before being cloned into the pENTR-vector by BP recombination (Invitrogen) following the manufacturer's instructions.

2.3.2 Transactivation assays

For the transactivation assays, 20 000 HEK293T cells were seeded on 96-well plates one day prior to transfection. The CMV-Tbx1 plasmids (10ng-40ng) either alone or in combination with the CMV-ptdsr construct (0ng - 40ng), was cotransfected with the 0.9 Pitx2 reporter construct (50ng) as well as with the CMV-renilla plasmid (10ng) using Fugene HD (Promega) following the manufacturer's instructions. The cells were then incubated for 24h at 37 degrees. After 6h serum starvation at 37 degrees, the cells were washed with PBS and lysed at RT in 100ul lysis buffer (25 mM Tris Phosphate Buffer pH 7.8, 2 mM CDTA, 10% glycerol and 1% Triton X-100). Firefly and Renilla Luminescence were measured sequentially. First, Firefly luciferase activity was measured using 10ul of the lysate in 100ul luciferase assay buffer (10 µg Potassium Luciferin, 15 mM MgSO4, 15 mM Potassium Phosphate Buffer pH 7.8, 4 mM EGTA pH 7.8, 20 µM ATP and 2 µM DTT). Luminescence was detected using a POLARstar Omega luminometer (BMG). Then renilla luciferase activity was measured by adding 100ul of PBS containing 10 µM of benzyl coelenterazine and 25 mM of Luciferase Inhibitor I (Merk Chemicals) to inhibit the firefly luminescence. Fluc and Rluc activities were measured as relative light units with a POLARstar Omega luminometer (BMG). The values of firefly luciferase activity were normalized for transfection using the renilla luciferase activity values.

Each experiment represents the average of 3 repeats and the final results represent the average of at least three independent experiments.

2.3.3 Protein Complementation Assays

For PCA assay, the two proteins of interest were fused to the first and second half of renilla luciferase using Gateway LR cloning. Both constructs (45ng of each) were cotransfected into 60% confluent HEK293T cells grown in 96-well plates using Fugene HD (Promega) following the manufacturer's instructions. In addition, a CMV-lacZ construct (10ng) was also contransfected to normalise for transfection efficiency and cell number. After 24h incubation at 37 degrees, the cells were washed with PBS and the renilla activity was measured in living cells in 100ul PBS by adding an additional 100ul PBS containing 10 µM of benzyl coelenterazine. The cells were then lysed at RT by adding 50 ul of 5x lysis buffer (125 mM Tris Phosphate Buffer pH 7.8, 10 mM CDTA, 50% glycerol and 5% Triton X-100). The LacZ assay was performed using 10ul of the lysate and adding 100ul LacZ buffer (16 mM Na2HPO4.7H2O, 40 mM NaH2PO4.H2O, 10 mM KCL, 1mM MgSO4) containing 10% of 10x OMPG and 0.27% Betamercaptoethanol. The lysate was incubated at 37 degrees protected from light until the appearance of yellow colour. The reaction was then blocked by adding 50ul 1M Na2CO3. The absorbance was measured with a POLARstar Omega luminometer (BMG). The values of renilla luciferase activity were normalized for transfection using the lacZ absorbance values.

Each experiment represents the average of 3 repeats and the final results represent the average of at least three independent experiments.

2.3.4 Lumier Assays

HEK293T cells were cultured in 96-well plates until 50% confluent and transfected with 50 ng of each construct (one tagged with His, the other one tagged with renilla luciferase) using Fugene HD (Promega) following the manufacturer's instructions. After 24h incubation at 37 degrees, the cells were washed with PBS and lysed for 1h in 150ul of 0.5% TNT (50mM Tris-HCl pH 7.4, 150 nM NaCl and 0.5% Triton X-100) containing cOmplete, EDTA-free protease inhibitor (Roche). 90ul of lysate was then transferred into a plate containing 10ul of paramagnetic Co coated beads. The lysate was incubated with the beads for 1h at 4 degrees with constant shaking. The beads were then washed 5 times with 200ul 0.1% TNT using a magnet to collect the beads at the bottom of the plate after each wash. After the last wash, 70ul of 0.1% TNT was added to the wells and the renilla luciferase activity was measured with a POLARstar Omega luminometer (BMG) after injecting 20ul 0.1% TNT containing 10 µM of benzyl coelenterazine.

CHAPTER 3

Effect of maternal preconceptional high-fat diet on the cardiac development of the offspring

3.1 Rationale for investigating the effect of maternal high fat diet on DiGeorge phenotype

With the currently increasing levels of obesity, especially in women of childbearing age, it is important to understand the consequences of this disease for the offspring. Increased prevalence of congenital anomalies, especially cardiac malformations in offspring from diabetic and obese mothers have been reported in several studies[37,132]. In mice, it has been shown that maternal high fat diet dramatically enhances the penetrance of laterality defects in *Cited2* deficient embryos[131]. To understand if the effect of preconceptional maternal high fat diet was affecting a wide range of cardiac development processes or whether it was specific to left/right patterning, it was decided to investigate whether preconceptional high-fat diet also affected the penetrance and severity of cardiac defects in the DiGeorge mouse model (*Df1/+*). As the cardiac defects observed in the DiGeorge model are related to abnormal neural crest cell migration and survival resulting from anomalous pharyngeal arch development[88,133], this would provide important information regarding the specificity of the effect of maternal obesity

as well as the possible underlying mechanism. Moreover, this study would shed some light on whether obesity may disrupt protective buffering mechanisms associated with the variable penetrance of congenital heart malformations found in DiGeorge Syndrome.

Mouse models are indeed very powerful tools to understand mechanisms underlying human disease and specifically congenital heart abnormalities. This is mainly due to the shared cardiac anatomy, including four chamber as well as a pulmonary and a systemic blood circulation, and physiology as well as the associated possible cardiac malformations such as septal defects, aortic arch and outflow tract malformations. An additional factor making mice such an attractive model is the phylogenetic closeness of the two species which, thanks to the availability of complete genomic sequences for both, makes the identification and understanding of the implicated cardiac genes remarkably easier. For example, the role of several important cardiac genes such as *TBX1*[23], *TBX20*[30], *NKX2.5*[19] and *GATA4*[21] in human congenital heart disease has been revealed through their study in mice.

The understanding of the mechanisms linking environmental factors, such as obesity to an increased prevalence of Congenital heart malformations could possibly give rise to new therapeutic strategies to prevent these anomalies by modifying the in utero environment. This could be achieved through simple measures such as the administration of food-supplements

and the change of certain habits during the early stages of pregnancy. For example, apart from the well know positive effect of folic acid on embryonic development, it has been suggested that the admisnistration of antioxidant agents such as vitamin C and E decreased embryonic dysmorphogenesis in diabetic rats[134-136].

3.2 Results

With the currently increasing levels obesity, especially in women of childbearing age, this study aimed to determine whether high-fat maternal diet has an effect on congenital heart malformations in a mammalian model. Work from our lab showed that maternal high-fat diet dramatically enhances the penetrance of laterality defects in *Cited2* deficient embryos. Here we investigate whether preconceptional high-fat diet affects the penetrance and severity of cardiac defects in a DiGeorge mouse model (*Df1/+*), where the cardiac defects are related to abnormal pharyngeal arch and neural crest cell development.

3.2.1 Power Calculation

The penetrance of cardiovascular defects in *Df1/+* mice has been reported to be ~30%[71,73]. Taking into account background variation, we estimated that in C57BL6/J wild-type mothers fed on a standard chow diet (control diet), the frequency of aortic arch and outflow tract defects in *Df1/+* embryos would be 20%. For this experiment, an enhancement effect of 20% was being taken as evidence of a biologically significant diet-*Df1* interaction. To detect an increase in aortic arch and outflow tract malformations in *Df1/+* embryos from 20% to 40% with power 0.8 and $p<0.05$, we had to examine 91 embryos in each group (i.e. control diet-fed and high-fat diet-fed). The power calculation uses binomial distribution Fisher's exact test

(one-sided). To obtain 91 *Df1/+* embryos per group, a total of 65 female mice were time mated.

3.2.2 High-fat diet results in obesity but not in hyperglycemia

Following 8 weeks on the diet, we found that C57BL6/J wild-type females were significantly heavier ($p<0.01$) but there was no significant difference in blood glucose levels. Control and high-fat diet wild-type female mice were mated to male *Df1/+* mice and the embryos were dissected out at 15.5 dpc (Figure 4 and 5). The data is summarized in Table 3. The litters of high-fat diet females were smaller than the litters of control diet females (Control diet 8.2 embryos; High-fat diet 6.3 embryos). There was no effect of high-fat diet on wild-type: *Df1/+* embryo genotype ratios (control 100:99, high-fat 91:93).

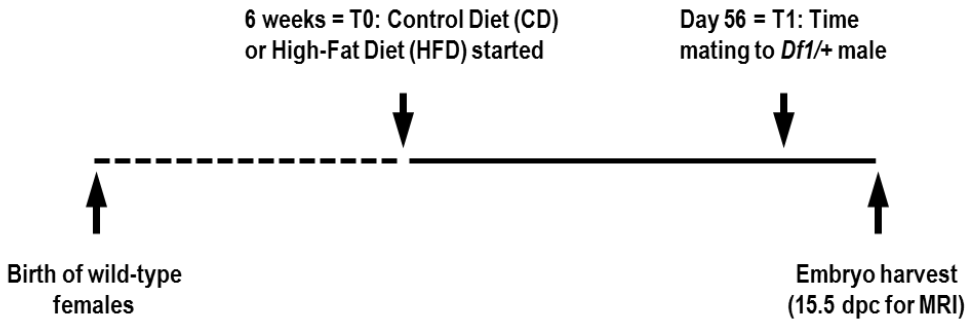

Figure 4. Experimental design: 6 week-old wild type females were put on either control diet (CD) or on high-fat diet (HFD) at T0. Time mating with *Df1/+* males were started at day 56 (T1). Embryos for MRI were collected at 15.5 dpc.

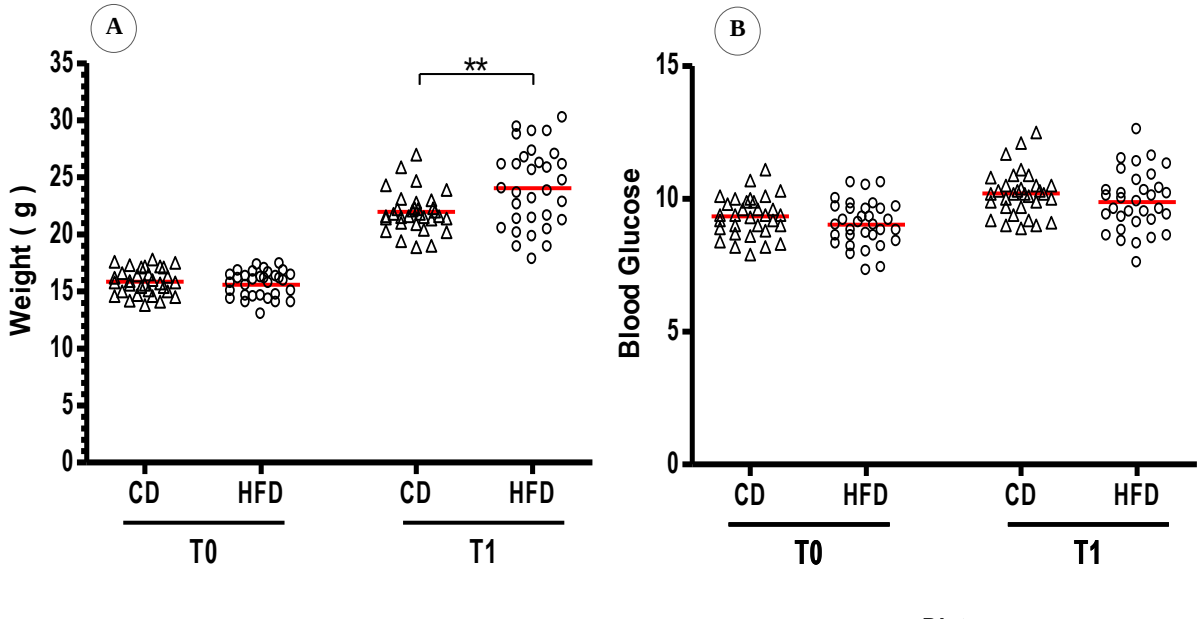

Figure 5. Effect of maternal high-fat diet on maternal weight (A) and fasting blood glucose (B). Weight and fasting glucose level by diet (CD or HFD) at time-point day 0 (T0) or day 56 (T1). (** = $p < 0.01$). Mean is indicated in red.

	CD		HFD	
	T0	T1	T0	T1
Weigth (g)				
Number of values	32	32	33	33
Mean	15.86	21.98	15.65	24.25
SEM	0.20	0.31	0.20	0.63
Glucose (mmol l^{-1})				
Number of values	32	32	33	33
Mean	9.34	10.29	9.04	9.88
SEM	0.13	0.15	0.15	0.20

Table 3. Summary of maternal weight and blood glucose data.

3.2.3 Maternal high-fat diet does not affect the penetrance or the severity of heart defects in Df1/+ embryos

To determine the effect of maternal high-fat diet on the penetrance and severity of heart defects in *Df1* deficiency, we examined embryos by MRI. The data is summarized in Table 4. In the high-fat group, cardiac defects (including ventricular septal defect , interrupted aortic arch, right sided aortic arch, vascular ring and common arterial trunk) occurred in 26 of 93 *Df1/+* embryos (28%) compared to 22 of 99 *Df1/+* embryos (22%) in the control diet group (Figure 6). These defects were observed in 9 of 91 wild-type embryos (10%) from the high-fat diet group and in 3 of 100 wild-type embryos (3%) from the control diet group. Thus, the penetrance of cardiac defects in *Df1/+* embryos is not significantly different between the two diet groups (p-value=0.363; Student's t-test). Although no increase in the frequency of total cardiac defects could be observed between the two diet groups, the frequency of VSDs in HFD embryos of each genotype was significantly higher compared to CD embryos (p-value < 0.01). This apparent 2.3 fold increase in the frequency of VSDs is most probably linked to the low embryonic weight of the affected embryos. Therefore this observation could be a consequence of embryonic growth retardation due to maternal obesity[137]. No difference in the severity of cardiac defects was observed between the two diet groups.

Phenotype	CD wt	HFD wt	CD Df1+/-	HFD Df1+/-
Ventricular septal defect	3	8	7	17
Common arterial trunk	0	0	0	0
Interrupted aortic arch	0	1	9	6
Right-sided aortic arch	0	1	2	0
Vascular ring	0	0	5	4
Number of embryo with HD	3	9	22	26
Total number of embryos	100	91	99	93

Table 4. Phenotypes observed by magnetic resonance imaging in wild-type and *Df1*/+ embryos on control and high-fat diets (CD and HFD).

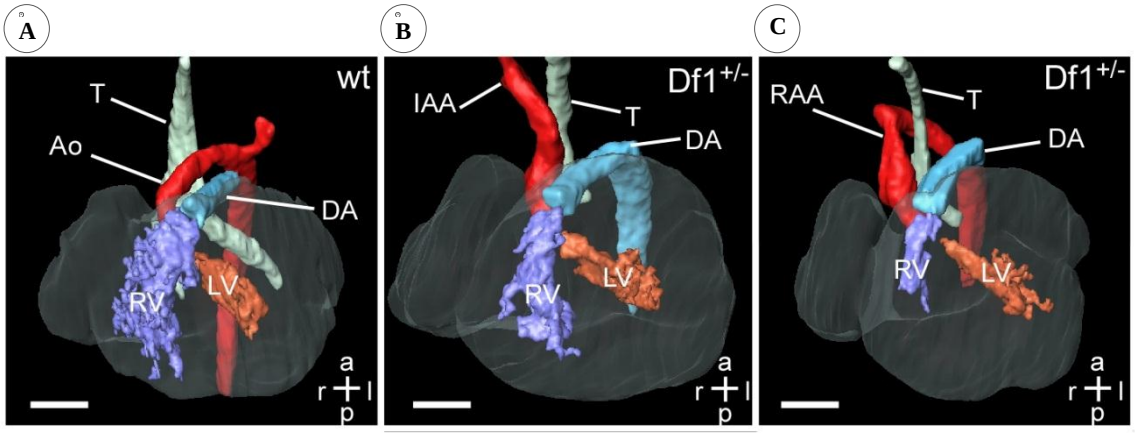

Figure 6. Heart malformations found in *Df1* deficient embryos at 15.5 dpc analysed using MRI. A) 3D reconstruction of a wild-type heart. The left ventricle (LV) gives rise to the Aorta (Ao). The right ventricle (RV) gives rise to the Ductus arteriosus (DA) which communicates whit the Aorta. The trachea (T) is indicated. B) 3D reconstruction of a *Df1*/+ embryonic heart from a high-fat diet mother. The Aorta (Ao) is interrupted and does not join the Ductus arteriosus (DA). C) 3D reconstruction of *Df1*/+ embryonic heart from a high-fat diet mother. The Ao goes to the right side of the trachea (RAA) and forms a vascular ring by joining the Ductus Arterious (DA).

3.2.4 Maternal high-fat diet affects thymus development and embryonic weight

The effect of high-fat diet on thymus size was explored using volumes measured from MRI data sets. The thymus size was corrected for embryo weight. We found that both diet and genotype affected thymus size but no genotype-diet interaction was observed (two-way ANOVA). Specifically we found that thymus volumes were significantly reduced by loss of the Df1 region ($p<0.001$) or by high-fat diet ($p<0.001$) (Figure 7B).

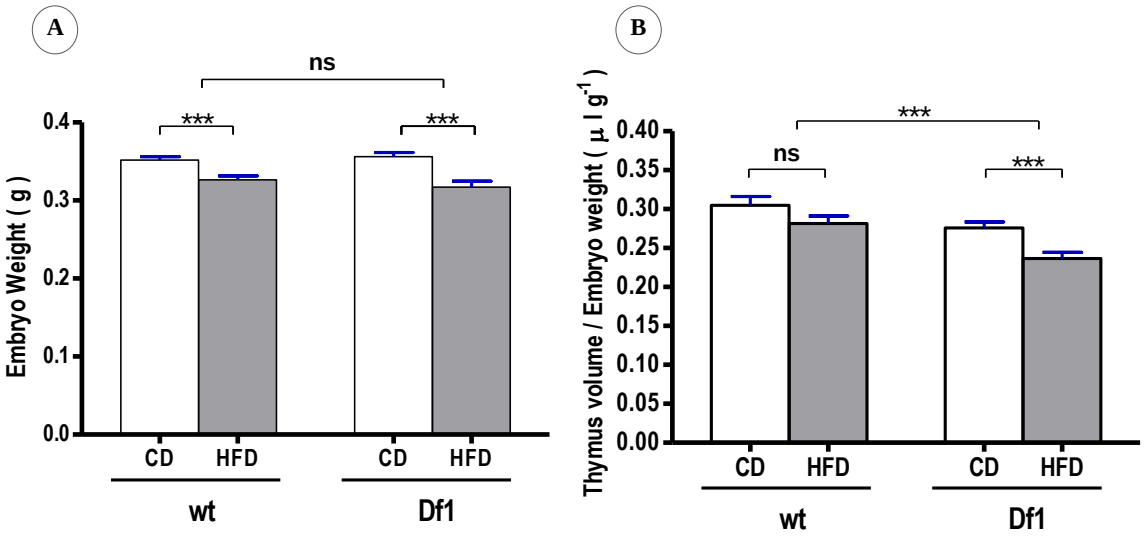

Figure 7. Effect of genotype and maternal diet on embryo weight (A) and thymus volumes (corrected for embryo weight). (B). Data is shown as mean ± standard error. (*** = $p<0.001$, ** =$p<0.01$, ns = non-significant).

The loss of *Df1* region did not reduce the embryo weight significantly. However, high-fat diet embryos were significantly lighter than control-diet embryos ($p<001$). No genotype-diet

interaction was observed (Two-way ANOVA) (Figure 7A)**.** The data is summarized in Table 5.

	wt		Df1+/-	
	CD	**HFD**	**CD**	**HFD**
Weigth (g)				
Number of values	100	91	99	93
Mean	0.35	0.33	0.36	0.32
SEM	0.00	0.01	0.01	0.01
Thymus volume ($\mu l\ g^{-1}$)				
Number of values	48	34	56	52
Mean	0.31	0.28	0.28	0.24
SEM	0.01	0.11	0.01	0.01

Table 5. Results summary of the effect of genotype and maternal diet on embryo weight and thymus volumes**.**

3.3 Discussion

3.3.1 Importance of understanding the effect of maternal HFD on embryonic development

The experimental design of this study was chosen to mimic the high-fat, calorically dense diet that is linked to the epidemic of human obesity in Western countries. The only difference between the control and experimental diets used in this study is the nutritional source which shifts from starch in CD to lard in the high fat diet. Understanding the effect of maternal obesity on the risk and severity of cardiac malformations in the offspring would allow us to develop preventative strategies, such as the use of a specific amount of vitamins, to reduce the incidence of congenital heart disease. A well-known example of such preventative measures is the intake of folic acid to avoid neural tube defects. The *in utero* environment which can be affected, for example, by maternal nutrition may disrupt the buffering mechanisms in developmentally protective networks to result in cardiac malformations.

3.3.2 Maternal HFD does not affect the incidence and severity of cardiac malformations in Df1/+ embryos

The observations made in this study convincingly demonstrate that maternal high-fat diet does not significantly affect the penetrance or severity of congenital heart defects in a DiGeorge mouse model. 28% of *Df1/+* HFD embryos showed heart malformations compared to 22% CD embryos of the same genotype. The same malformations were observed for both diets including VSD, IAA, RAA and VR.

These results are particularly interesting when compared to those obtained in a similar study assessing the interaction of maternal high-fat diet and embryonic *Cited2* deficiency [131]. The study demonstrated that there was a significant increase in the penetrance of left-right patterning defects in HFD *Cited2*$^{-/-}$ embryos when compared to CD embryos of the same genotype. There are different possible explanations for the discrepancy of the effect of maternal HFD on embryonic *Cited2* and *Df1* phenotype. First, the difference might be associated with the different nature of the developmental processes (left/right patterning versus neural crest cell migration), involving a separate set of genes and associated pathways, affected by the loss of *Cited2* or *Df1*. Second, *Cited2* and *Tbx1* are expressed at different time points, which could make their function more or less susceptible to be affected by environmental factors. *Cited2* is expressed very early during development at the time when left-right patterning is established mainly through the Nodal pathway. It may be suggested that maternal HFD interacts with variants in the Nodal pathway genes,

such as *Alk4* and *Foxh1*, which in addition to the loss of *Cited2* weakens the system and results in cardiac malformations. As the genes involved act very early in development, a modification of their function that early might have a significant effect on all successive developmental processes. For instance, it has been reported on several occasions[138,139] that *Shh*, which is involved in the establishment of left-right patterning, is dependent on cholesterol to function properly. Considering that abnormal cholesterol metabolism has been associated with several human syndromes associated with cardiac malformations[140,141], this could provide a plausible explanation for the involvement of maternal high fat diet in CHD. On the other hand, *Tbx1*, being expressed later in development, is involved in much later events, specifically the development of the pharyngeal arches and neural crest cell migration and survival. It is possible that the disturbance of biological processes by environmental factors, such as maternal high fat diet, might affect proper development only marginally at this stage. This could be a reason why the left-right patterning network is especially susceptible to maternal HFD, whereas HFD does not appear to have a significant effect on the mechanisms controlling the neural crest cell survival and migration.

3.3.3 Maternal HFD affects the incidence of congenital malformations in wild-type embryos

The increased proportion of abnormal embryos in HFD wild-type embryos (10% abnormal HFD wt embryos vs 3% abnormal CD wt embryos) is an unusual result, as it has not been observed in other wild-type embryos subjected to HFD in previous studies.

One possible explanation for this phenomenon might reside in an effect of the *Df1* deletion on epigenetic modifications, such as methylation or acetylation, of DNA in sperm from *Df1*/+ males. As a result, the transmitted paternal wild-type allele may have an altered methylation/acetylation profile. A key experiment to show if there is a paternal epigenetic effect of the *Df1* deletion on the incidence of malformations in the offspring of HFD-fed mothers would be a cross between wt males and *Df1*/+ females put on HFD. Even if there might also be an effect of the *Df1* deletion on the epigenetic profile in the germline of these females, it might not affect embryonic development of wt embryos in the same way.

It has been suggested that T-box proteins, including those of the *Tbx1* subfamily may target chromatin and interact with modifying enzymes and could therefore have a role in epigenetic reprogramming events[124]. In this case, the loss of normal epigenetic patterns could be enough to tip the balance and make embryonic development more susceptible to the influence of environmental factors, such as high fat maternal diet. In order to test this hypothesis, one could envisage, for example, the addition of methyl donors to the diet which could reverse the observed increase in malformations in HFD wt embryos.

Similarly, the addition of acetyl donors may increase the proportion of abnormal HFD wt embryos even further. Of course, it is also possible that the opposite effects are observed.

Embryo transplant experiments at very early developmental stages could provide a better understanding of the interaction between epigenetic modifications and HFD. In this case, embryos from HFD fed mothers would be transplanted into CD fed mothers just after fertilisation and the incidence of malformations in wt embryos could then be compared to the incidence malformations in the embryos fertilised and developed in HFD fed mothers. If a similar proportion of abnormal embryos can be established, this would indicate that inherited epigenetic mechanisms are involved.

Finally, to quantify and understand how maternal HFD might affect epigenetic mechanism in embryos, the genome wide comparison of methylation and acetylation patterns in embryos coming from CD and HFD fed mothers would be crucial. Moreover the comparison of the methylation/acetylation profile between wt embryos coming from wt fathers with the methylation/acetylation profile found in embryos from the same genotype coming from *Df1* fathers would uncover a potential role of the *Df1* region in transmissible epigenetic processes. Methylated/Acetylated DNA immunoprecipitation chip based assay would be a very potent technique to address these questions.

3.3.4 Maternal HFD reduces embryo weight for all genotypes and loss of Df1 region reduced embryo weight even further

This study shows that maternal high-fat diet reduces embryo weight for all genotypes. Similar observations had been made in a previous environment-gene interaction study[131]. One possible explanation for this phenomenon is the Barker's "fetal origins" hypothesis which proposes that alterations in fetal nutrition result in developmental adaptations that permanently change structure, physiology and metabolism. The mother is thus providing her baby with a forecast of the environment in which it will be born. In cases where the forecast does not match the actual post-natal situation this may result in metabolic conflict and lead to cardiovascular, metabolic and endocrine disease in adult life[142-146]. The reduction in weight observed in HFD embryos might therefore be interpreted as a prevention of obesity in adult life.

This study also shows that embryos lacking the *Df1* region were significantly lighter than wild-type embryos, which could be associated to the general developmental delay in DiGeorge patients.

3.3.5 Maternal HFD reduced thymus volumes for all genotypes

The significant reduction in thymus volumes of HFD embryos, regardless of their genotype, has previously been observed in J. Bentham *et al.*[131], and suggests that HFD affects the expression of certain genes responsible for thymus development. Hypotrophic thymus was observed in all *Df1/+* embryos on either diet and is commonly considered one of the most sensitive indicators of TBX1 levels. However, it is not known whether the thymus size reduction by HFD and by the loss of the *Df1* region occurs through the same mechanism or through parallel pathways. The fact that no increase of CHD such as aortic arch and outflow tract defects was observed in *Df1/+* embryos, despite an increase in thymus defects, may suggest that the *Df1* model might not reduce TBX1 level enough for heart morphogenesis to be affected by external factors such as maternal high fat diet.

3.3.6 HFD increased maternal weight more in Cited2+/- females than in wt females

As already shown in previous studies[131], the high fat diet that we used in our study results in maternal weight gain as well as increased blood glucose levels. Whereas the blood glucose level increase observed in the present experiment was the same as what was previously observed in the study assessing the interaction between maternal HFD and loss of *Cited2*, the weight increase in the mothers was significantly higher in *Cited2* heterozygous females compared to the wild-type females used in this study. This observation would suggest that *Cited2* may have a role in metabolism and given that the

loss of one copy of *Cited2* renders the females more susceptible to become obese under HFD conditions.

3.3.7 Choice of the Df1 mouse model

In this study, the *Df1* murine model was chosen to study the effect of preconceptional maternal high fat diet on the DiGeorge phenotype. The reason why this model was preferred over the $Tbx1^{+/-}$ mouse model resides in its genetic and phenotypic resemblance to the human Syndrome. Not only does the *Df1* mouse phenocopy the complete human DiGeorge phenotype but the underlying cause of the phenotype is a deletion in both cases. However, there are some difficulties associated with this choice of murine model. First of all, it is impossible to assign any observed effect of maternal diet to the reduction of Tbx1 exclusively as there are several other genes included in the *Df1* deletion. Second, with regards to the results obtained in this study, it might be hypothesised that the *Df1* model is too robust to detect any effect of environmental factors such as maternal diet on the offspring phenotype. Maternal high fat diet may not be enough to tip the balance in a detectable way in this model on a C57B6J background. Alternatively, the $Tbx1^{Neo2/Neo}$ model[73] may have been a better suited model to study the effect of maternal high fat diet as the level of *Tbx1* expression lies at the threshold of normal phenotype. It is characterized by a *Tbx1* expression of around 20% and has a highly variable phenotype, especially those associated with the outflow tract, which could be more prone to variability under the influence of environmental factors. However, it is important to keep in mind that the

defects associated with DiGeorge syndrome are closely linked to the level of TBX1 activity and different phenotypic features have variable sensitivity to TBX1 levels. Therefore, another possible model would have been the *Tbx1*$^{+/Neo}$ mouse which has only 50% of the normal TBX1 activity. This model would have been more suitable to detect subtle variation in aortic arch abnormalities. Each of the models cited above is suitable for the study of specific aspects of the DiGeorge Syndrome phenotype and none of them covers the whole spectrum of phenotypes. The best option may therefore have been to use all three of them for this study, which was not possible due to the number of mice that would have been needed and to financial constraints.

CHAPTER 4

George, a novel ENU induced mutation in Tbx1

4.1 Rationale to characterize an ENU mutant with DiGeorge phenotype

In humans, resequencing of candidate genes in patients is the most common way to discover functional domains of specific proteins. Several *TBX1* point mutations have been found in DGS patient cohort screening and have uncovered functional domains of the TBX1 protein, such as the nuclear localisation signal[24,69,147,148].

In mice, Ethylnitrosourea (ENU) induced mutagenesis targets premeiotic spermatogonial stem cells by introducing point mutations and can produce different types of alleles, for example, loss of function mutations, hypomorphs, antimorphs and even gain of function mutations. By altering subtly individual protein domains and splicing products, ENU mutagenesis is ideally suited to reveal discrete unknown functions of specific proteins of interest.

The discovery of a mouse mutant showing the complete DiGeorge phenotype during a phenotype-driven recessive ENU screen in our laboratory was accompanied by the

possibility of getting a better understanding of the molecular mechanisms underlying DiGeorge Syndrome. The characterization of this mutant could result in two different scenarios: first, the point mutation could be located in the *Tbx1* gene. This would provide an opportunity to investigate *Tbx1* function as well as to identify some key functional domains or residues in the TBX1 protein. Second, the mutation could be found in another gene which may lead to the identification of a new candidate gene involved in DGS.

4.2 Results

4.2.1 George: a novel recessive ENU mutant with DiGeorge features

Through the ENU mutagenesis screen, several embryos with consistent externally visible features, including severe oedema and red blisters under the skin were identified. The analysis of these embryos by MRI showed that they had cleft palate, absent cochlea, absent thymus and cardiac malformations, including interrupted aortic arch, vascular ring, right sided aortic arch, common arterial trunk and ventricular septal defects. All of these malformations are typically found in DiGeorge syndrome. As point mutations confer unique insight into protein function, we further characterized this mutation.

4.2.2 George results from a mutation in the highly conserved Tbx1 T-box domain with potential effect on protein structure and function

Dr. Dorota Szumska mapped the mutation to a minimal segregating interval of 25Mb between rs4161352 and D16Mit112 containing almost 200 genes. As *Tbx1* lies in this interval and the phenotype completely overlaps the phenotype found in *Tbx1*$^{-/-}$, *Tbx1* was considered to be the most likely candidate gene. Therefore, all the *Tbx1* exons were sequenced. We identified a G/A transition at the very end of *Tbx1* exon 3 (Figure 8).

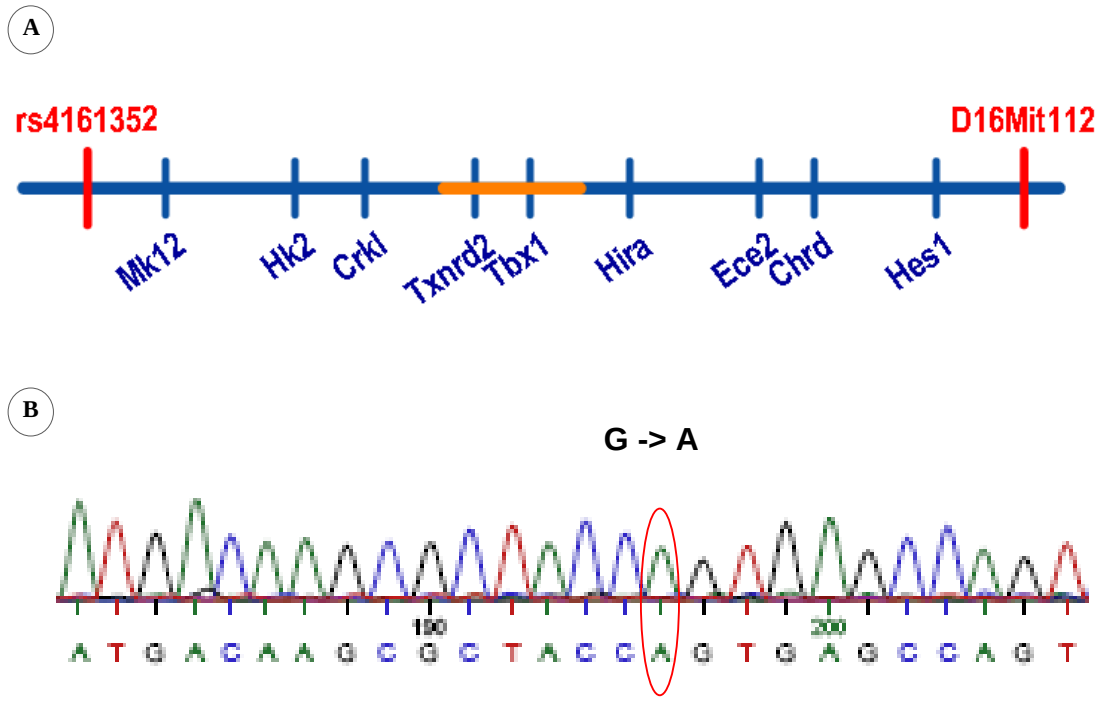

Figure 8. Mapping and identification of the George mutation. A) Map of Chr 16 showing the minimal C57BL/6 interval between rs4161352 and D16Mit112 (Chr16: 10874116 - 35128571) that segregated with the phenotype. Cardiac genes located in this interval are also indicated. The *Df1* deletion region is indicated in orange. B) Sequencing chromatogram of *Tbx1* showing the end of exon 3 and the beginning of the following intron from an affected embryo showing a homozygous G -> A transition.

4.2.3 George does not complement a Tbx1 null allele

To determine whether the George mutation is indeed a new allele of *Tbx1*, we performed a complementation test by crossing it to the $Tbx1^{tm1Bld}$ null allele. The phenotypes of single heterozygous embryos and embryos carrying both alleles were analysed by MRI. We found that embryos carrying both alleles ($Tbx1^{-/Geo}$) completely recapitulated the $Tbx1^{Geo/Geo}$ as well as the previously published $Tbx1^{-/-}$ phenotype[22,72] in all embryos studied (12 out of 12). All $Tbx1^{-/Geo}$ embryos had severe oedema, red blisters under the skin, cleft palate, hypotrophic to absent thymus and cardiac defects including interrupted aortic arch, vascular ring, right sided aortic arch, common arterial trunk and ventricular septal defect. Cardiac defects were observed in 2 of 10 $Tbx1^{+/Geo}$ embryos. No abnormalities were observed in $Tbx1^{+/-}$ and wild-type littermate embryos (Figure 9 and Figure 10). The data is summarized in Table 6.

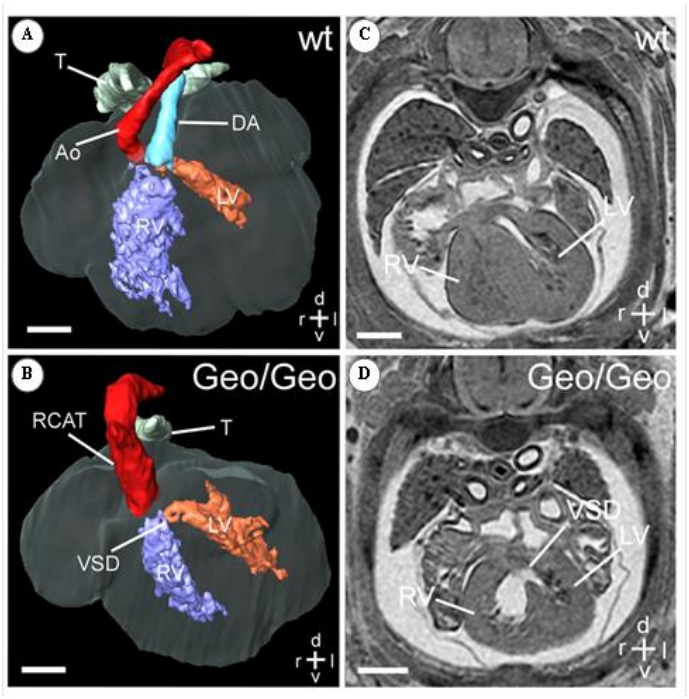

Figure 9. Heart malformations found in *Tbx1*$^{Geo/Geo}$ embryos at 15.5 dpc analyzed via MRI. A) 3D reconstruction of a wild-type heart (wt). Left ventricle (LV), right ventricle (RV), Aorta (Ao), ductus arteriosus (DA) and trachea (T) are indicated. B) 3D reconstruction of a *Tbx1*$^{Geo/Geo}$ embryonic heart. The left ventricle (LV) and the right ventricle (RV) communicate due to an outflow ventricular septal defect (VSD). The right ventricle gives rise to a common arterial trunk (RCAT) going to the right of the trachea (T). C) Transverse section through a wt embryo heart. Left (LV) and right ventricle (RV) are indicated. D) Transverse section through a *Tbx1*$^{Geo/Geo}$ embryo heart. The ventricles communicate through a ventricular septal defect (VSD).

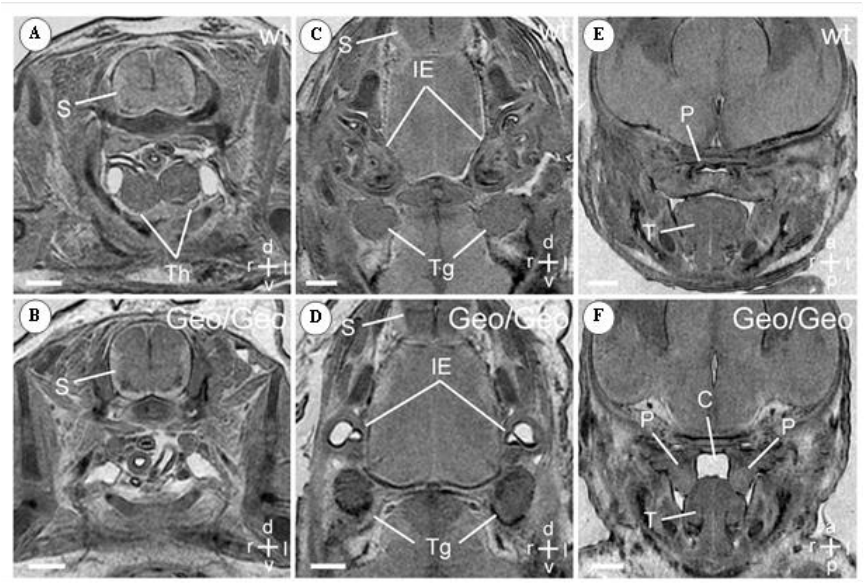

Figure 10. Non-cardiac malformations found in *Tbx1*$^{Geo/Geo}$ embryos at 15.5 dpc analyzed via MRI. A) Transverse section through a wt embryo. Spine (S) and thymus lobes are indicated (Th). B) Transverse section through a *Tbx1*$^{Geo/Geo}$ embryo. Thymus is absent. C) Transverse section through a wt embryo head. Inner ear (IE) contains the cochlea; Trigeminal (Tg) is also indicated. D) Transverse section through a *Tbx1*$^{Geo/Geo}$ embryo head. The cochlea is absent. E) Sagittal section of a wt embryo. Palate (P) and tongue (T) are indicated. F) Sagittal section of a *Tbx1*$^{Geo/Geo}$ embryo. Palate is cleft (C).

Phenotype	Tbx1$^{-/Geo}$	Tbx1$^{+/Geo}$	Tbx1$^{+/-}$
Ventricular septal defect	8	0	0
Common arterial trunk	10	0	0
Interrupted aortic arch	0	0	0
Right-sided aortic arch	4	0	0
Vascular ring	1	2	0
Resorptions	2	0	0
Number of embryos with HD	12	2	0
Total number of embryos	12	10	10

Table 6. Complementation test results. Phenotypes observed by MRI in *Tbx1*$^{-/Geo}$, *Tbx1*$^{+/Geo}$ and *Tbx1*$^{+/-}$ embryos. George fails to complement a *Tbx1* null allele.

4.2.4 George affects splicing of Tbx1 mRNA

Since the George mutation is located in the splicing donor region at the end of exon 3, it is therefore predicted to potentially disrupt the splicing factor recognition sequence. Based on the sequence, three different transcripts were expected: i) transcript containing G>A point mutation resulting in a R160Q amino acid substitution, ii) transcript lacking exon 3 and iii) transcript retaining intron 3 resulting in a truncated protein. Splicing of *Tbx1* was examined in wild-type, heterozygous ($Tbx1^{+/Geo}$) and homozygous mutant ($Tbx1^{Geo/Geo}$) 10.5dpc embryos by RT-PCR followed by sequencing of the PCR products (Figure 11). PCR between exon 2 and exon 5 produced a 500nt fragment for wild-type embryos and a 398nt fragment for $Tbx1^{Geo/Geo}$ embryos. $Tbx1^{+/Geo}$ embryos had both fragments. Sequencing of the 398nt fragment showed that exon 3 was skipped in frame.

Gel electrophoresis showed that the intensity of the 398bp band in $Tbx1^{Geo/Geo}$ embryos was much lower than any of the bands in $Tbx1^{+/Geo}$ or wild-type embryos.

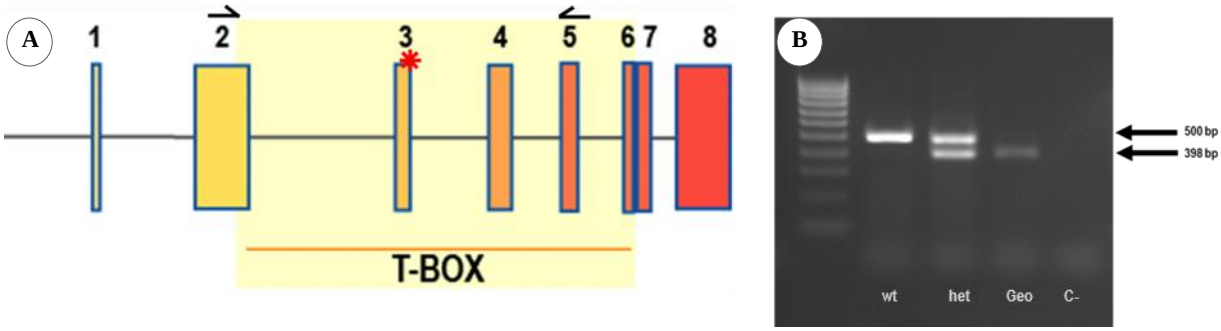

Figure 11. George mutation affects correct splicing of *Tbx1* mRNA. A) Genomic structure of *Tbx1*. Primer positions used for RT-PCR are indicated. B) RT-PCR products from wild-type, $Tbx1^{+/Geo}$ (het) and $Tbx1^{Geo/Geo}$ (Geo) embryos at 10.5 dpc. Sequencing of these RT-PCR products revealed that the lower band corresponded to *Tbx1* mRNA lacking exon3.

4.2.5 George phenotype is caused by the absence of TBX1

To study the effect of the George mutation on *Tbx1* expression, proteins were extracted from wild-type, heterozygous ($Tbx1^{+/Geo}$) and homozygous mutant ($Tbx1^{Geo/Geo}$) 10.5dpc pharyngeal arches. $Tbx1^{-/-}$ pharyngeal arch protein extracts were used as negative control. As expected, wild-type TBX1 could be detected at k52 Da in $Tbx^{+/+}$ and $Tbx1^{+/Geo}$ protein extracts whereas all of the variants were below detection level in the $Tbx1^{Geo/Geo}$ extract (Figure 12). This result implies that the George phenotype is due to the absence of TBX1. The George allele can therefore be considered as a new *Tbx1* strong hypomorph allele or a functionally null allele.

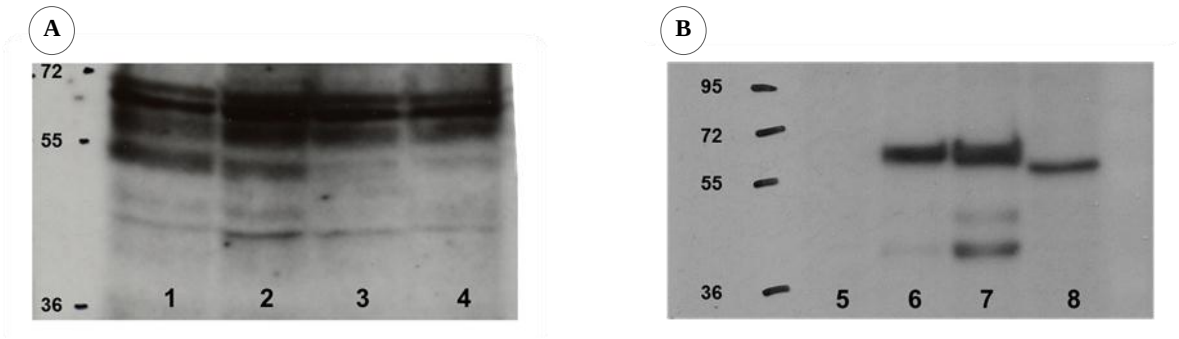

Figure 12. Western Blot showing expression of TBX1 variants in A) 10.5 dpc embryonic tissue; Lane1: wild-type; Lane2: *Tbx1*$^{+/Geo}$; Lane3: *Tbx1*$^{Geo/Geo}$; Lane4: *Tbx1*$^{-/-}$ (neg. control). B) Transiently transfected HEK293T; Lane5: untransfected cells (neg. control); Lane6: Wild-type TBX1; Lane7: TBX1 containing R160Q mutation; Lane8: TBX1 lacking exon 3.

4.2.5 The loss of exon 3, as opposed to the R160Q point mutation, does not affect Tbx1 transactivation capacity

As the deletion of exon 3 corresponds to the loss of 25% of the DNA-binding T-box domain, it was hypothesised that the TBX1 Ex3del variant would have strongly decreased transactivation capacity. Therefore, a luciferase assay with the TBX1 responsive 0.9Pitx2-fluc reporter containing two head-to-head palindromic T-box binding sites (T-half sites) was carried out in HEK293T cells. Increasing amounts of wild-type, R160Q *TBX1* and Ex3 del *TBX1*, ranging from 0 ng to 40 ng, were cotransfected with the 0.9 Pitx2-fluc reporter and luminescence was measured after starving the transfected cells for 12h. Results showed that the reporter was activated by wild-type and Ex3del TBX1 in a dose-dependent

manner. The measured relative luminescence increased from 2.34 to 5.12 between 10ng and 40ng wild-type *TBX1* and from 2.19 to 4.46 between 10ng and 40ng Ex3del *TBX1*. However, the R160Q TBX1 variant had very little effect at any dose and the measured luminescence ranged from 1.75 to 2.27 (Figure 13). The expression of all TBX1 variants was confirmed by Western Blot.

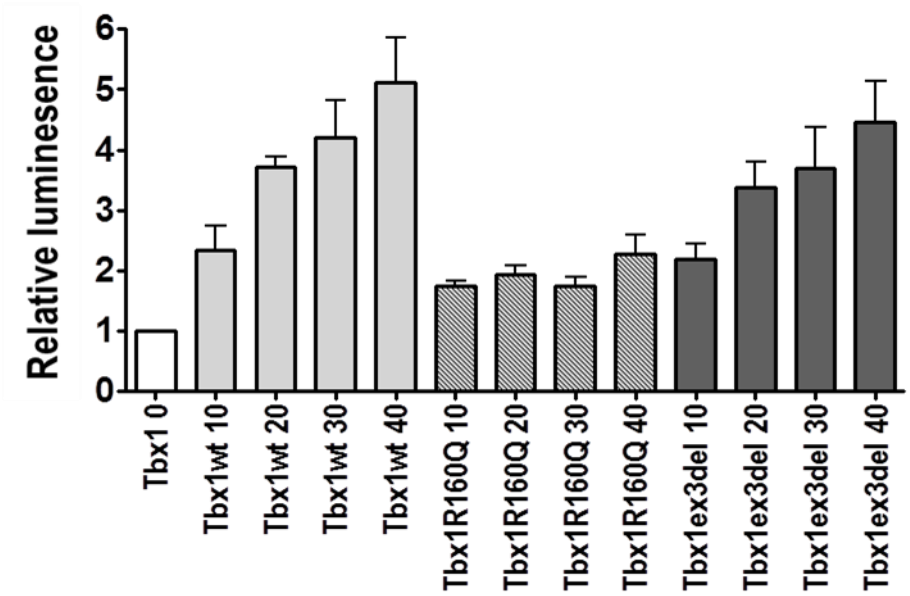

Figure 13. Transactivation capacity of wild-type TBX1, TBX1 R160Q and TBX1 Ex3del at *Pitx2* promoter. Increasing quantities of *TBX1* was transfected in HEK293T cells. Transactivation capacity of wild-type TBX1 increases proportionally with *TBX1* quantity (0-40ng) as assessed by total luciferase reporter activity. TBX1 R160Q shows very low transactivation and does not depend on the levels of plasmid transfected. TBX1 Ex3del retains transactivation capacity which increases proportionally to *TBX1* Ex3del quantity. Luminescence readings and standard error of mean are indicated.

This result shows that the exon 3 is not necessary for TBX1 transactivation capacity as the Ex3del variant does not seem to affect reporter luminescence significantly. Moreover, the

residue R160 seems to have a key role in *Tbx1* function. One possibility is that this residue is important for the proper folding of the TBX1 protein and the substitution of the arginine by a glutamine residue could lead to misfolding, rendering the protein unstable and less functional. However, prediction of the TBX1 R160Q T-box domain based on the crystallisation of the TBX1 wt T-box domain showed that this mutation had no effect on the 3 dimensional structure of the protein as opposed to the loss of exon 3 (K. El-Omari, personal communication) (Figure 14). Another possible explanation for the loss of transactivation capacity of the point mutant could be that the R160 residue is involved in the TBX1 - DNA interaction, due to its positive charge and its location in the DNA-binding T-box domain (K. El-Omari, personal communication). To explore the role of residue R160 in TBX1-DNA binding further, the DNA - binding affinity of wild-type and R160Q T-box was assessed through Surface Plasmon Resonance (Biacore®). Three different biotinylated double-stranded oligonucleotides were used: i) The TBX20 binding site containing one T-half site, ii) the putative TBX1 minimal binding site determined through SELEXA (P. Scambler, personal communication) containing two head-to-tail T-half sites and iii) the sequence that was used for the crystallization of the T-box containing two head-to-head T-half sites. Results showed wild-type and R160Q T-box bind to the TBX20 binding site containing one T-half site (i) and the two head-to-head T-half sites (iii) with a much higher affinity than to the two head-to-tail T-half sites (ii). Moreover, the R160Q variant has a higher dissociation constant (Kd) and therefore a lower affinity for the target DNA. The data is summarized in Table 7.

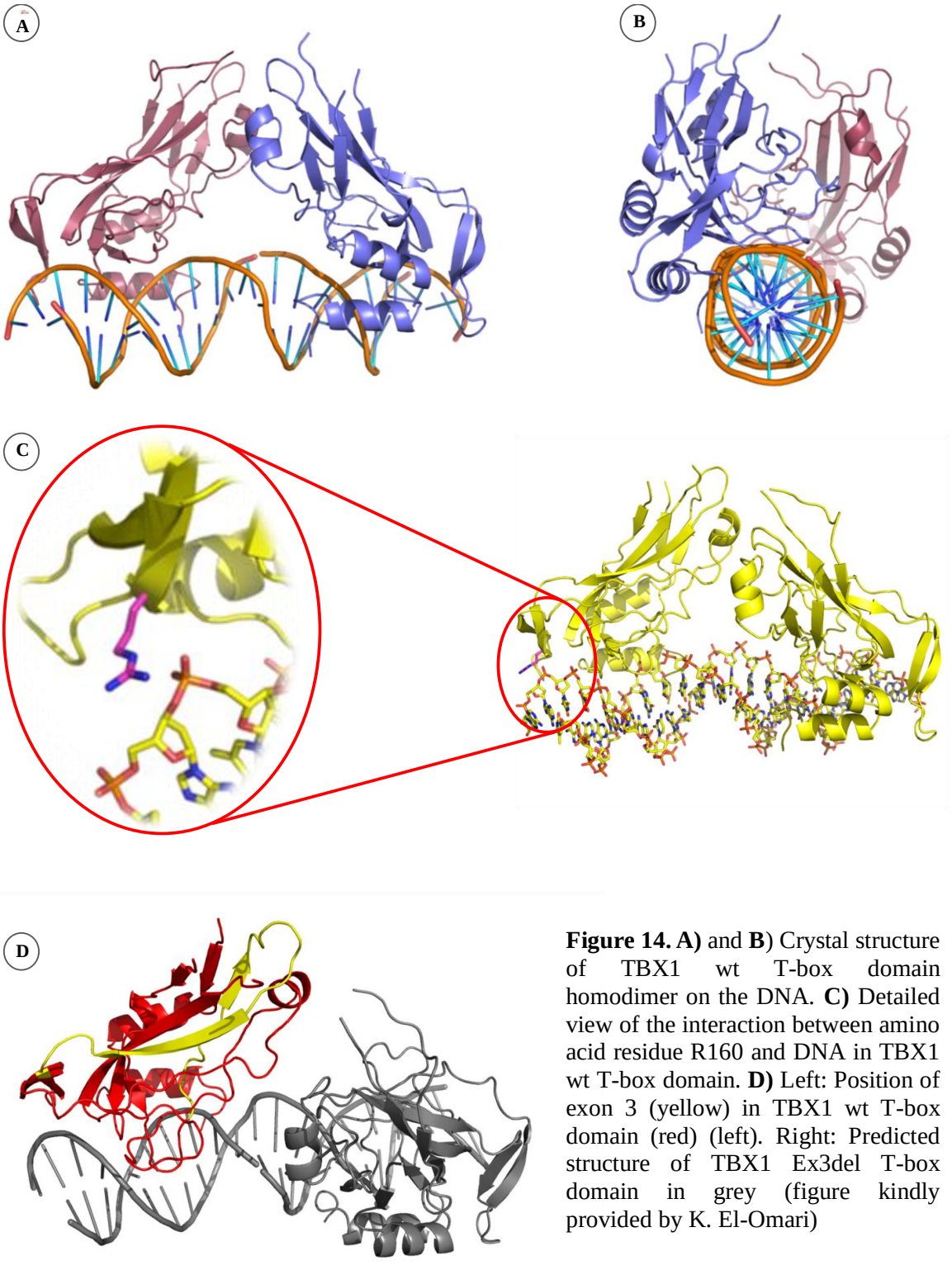

Figure 14. A) and **B**) Crystal structure of TBX1 wt T-box domain homodimer on the DNA. **C)** Detailed view of the interaction between amino acid residue R160 and DNA in TBX1 wt T-box domain. **D)** Left: Position of exon 3 (yellow) in TBX1 wt T-box domain (red) (left). Right: Predicted structure of TBX1 Ex3del T-box domain in grey (figure kindly provided by K. El-Omari)

	wt	R160Q	oligo sequence
single T-site	6.2 (1)	27.1 (7)	Biotin-CTCTTATAGGTGTGAAAACCGTG
head-to head	6.4 (2)	17 (1)	Biotin-GCTCTAATTTCACACCTAGGTGTGAAATTGCGCT
head-to-tail	600 (80)	120 (50)	Biotin-CTCTTCACACTTTCACACC

Table 7. Summary of Dissociation Constants (Kd) of wild-type and R160Q T-Box on different oligos measured by Surface Plasmon Resonance. Kd are measured in uM and error is indicated in (). T-half sites are underlined in the oligo sequences.

These results indicate that the residue R160 plays an important role for DNA binding and therefore contributes to the stable interaction between TBX1 and the target DNA.

Finally, the decrease in TBX1 transactivation capacity could also be due to the potentially essential role of the R160 residue in TBX1 homodimerization. Indeed, protein complementation assays were performed to study whether the R to Q amino acid substitution had an effect on the dimerization. Results obtained by PCA assay which will be discussed in the next chapter, showed that the R160Q mutation as well as the deletion of exon 3 reduced the dimerization "capacity" by 60%. Moreover, crystallisation experiments of the TBX1 wt T-box domain showed that independent binding of the two TBX1 monomers to the DNA was necessary prior to dimerization. Thus, the most probable explanation for the loss of transactivation capacity of the R160Q variant is the loss of stable TBX1 dimerization required for effective transactivation. However, this is very

likely to explain the loss of transactivation only partially as the same reduction of dimerization affinity is observed for the Ex3del variant, without such a significant effect on transactivation. Therefore, it might be a combined consequence of decreased DNA affinity and the inability to form stable homodimers.

4.2.6 George affects TBX1 cell localization

The inability of the TBX1 R160Q mutant to activate transcription from the 0.9 Pitx2-fluc reporter construct, suggests that this point mutation has resulted in the disruption of a key transactivation domain or that the protein is unstable, misfolded or does not translocate to the nucleus. Therefore the subcellular localization of the transfected TBX1 R160Q – mcherry fusion protein has been examined. It was found to localize to the nucleus like wild-type TBX1. In contrast, the TBX1 variant lacking exon 3 localized predominantly in the nucleus but it could also be detected outside of the nucleus maybe trapped in the Golgi or the ER. However, the fact that TBX1 Ex3del was able to transactivate in the luciferase reporter assay implies that there is a considerable amount of this variant in the nucleus. In conclusion, the lack of transactivation capacity of TBX1 R160Q is not due to a lack of TBX1 presence in the nucleus (Figure 15).

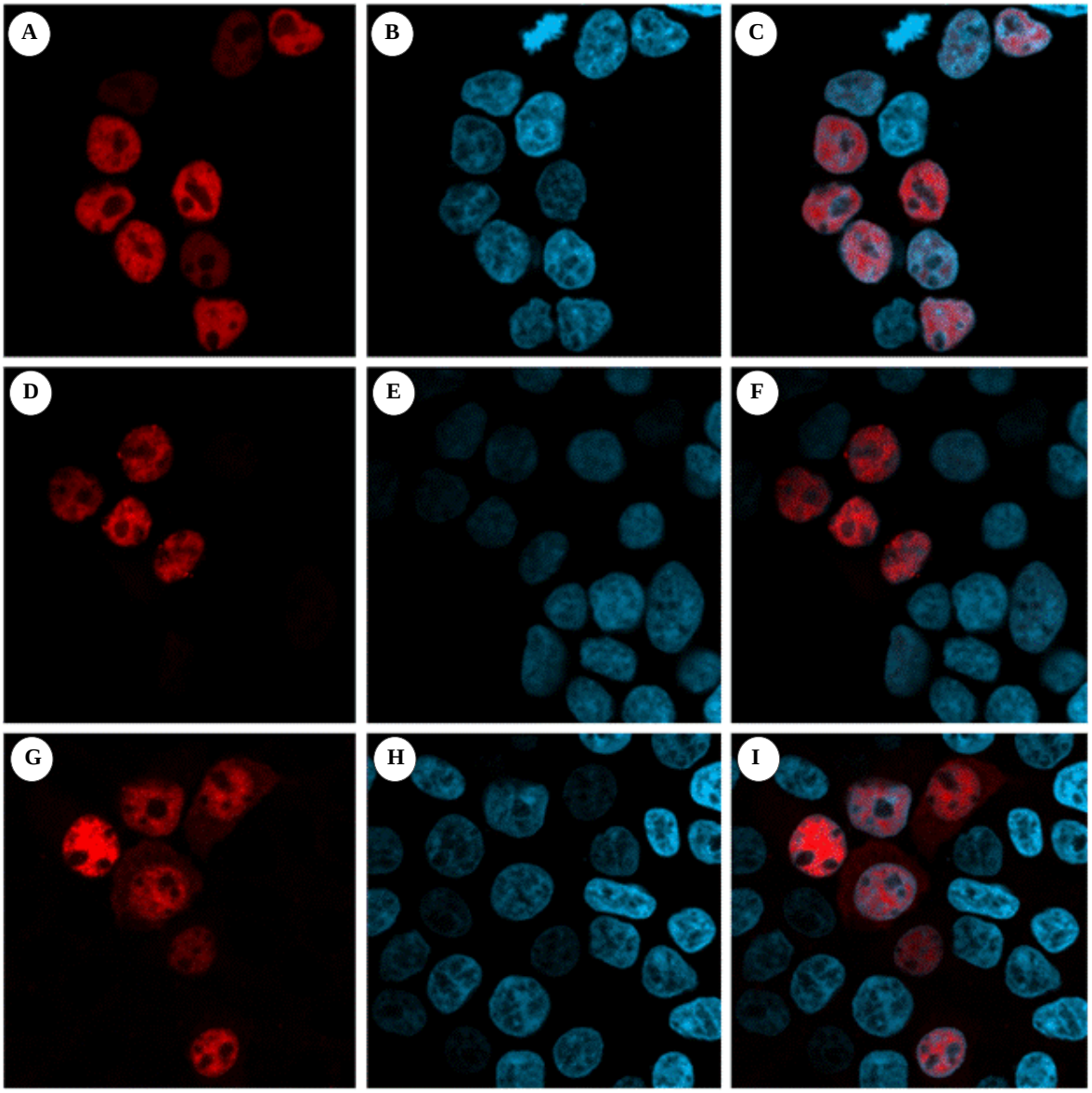

Figure 15. TBX1 localisation in HEK293T cells. **A) - C)** TBX1 wt localises to the nucleus: **A)** TBX1 wt –mcherry. **B)** DAPI staining of the nucleus. **C)** Merged images A) and B). **D – F)** TBX1 R160Q localises to the nucleus.: **D)** TBX1R160Q –mcherry. **E)** DAPI staining of the **nucleus. F)** Merged images D) and E). **G) – I)** TBX1 Ex3del localises to the nucleus but can also be detected outside the nucleus: **G)** TBX1 Ex3del –mcherry**. H)** DAPI staining of the nucleus.**I)** Merged images G) and H).

4.3 Discussion

TBX1 is considered to be responsible for most of the congenital abnormalities seen in DiGeorge Syndrome. It is the only gene for which mutations have been found in patients with the characteristic DGS phenotype but who lack the typical 3 Mb chromosomal deletion[69]. However, it cannot be ruled out, that the DG phenotype observed in these non-deleted patients is not entirely and exclusively due to the detected point mutation in *TBX1*. In theory, it could also result from a loss of buffering through mutations in other genes that are linked to the *TBX1* network. The observation that the cardiac phenotype is only partially penetrant in deleted patients could fit with this hypothesis.

A key unresolved issue is the molecular mechanism linking *TBX1* mutations to the disease. The study of point mutations is a very potent tool to address this question and may provide crucial information for understanding specific functions and roles of *TBX1* in the genetic network governing embryonic development.

The *George* mouse mutation was identified through an ENU screen and resulted in the complete DiGeorge phenotype when homozygous, including VSD, CAT, RAA and VR as well as cleft palate, hypoplastic to absent thymus, inner ear malformation and very severe oedema.

The *George* mutation was predicted to result in two altered protein products, an amino acid substitution and an in frame deletion of exon three. The amino acid substitution changes an Arginine to a Glutamine at position 160. As the R160Q mutation is located within the T-box domain, more specifically in the sequence PVDDKRY**R**YAFHSSS, which is completely conserved in the *Tbx1* superfamily, we hypothesized that this amino acid substitution could affect the function of the normally spliced TBX1 protein (Figure 16).

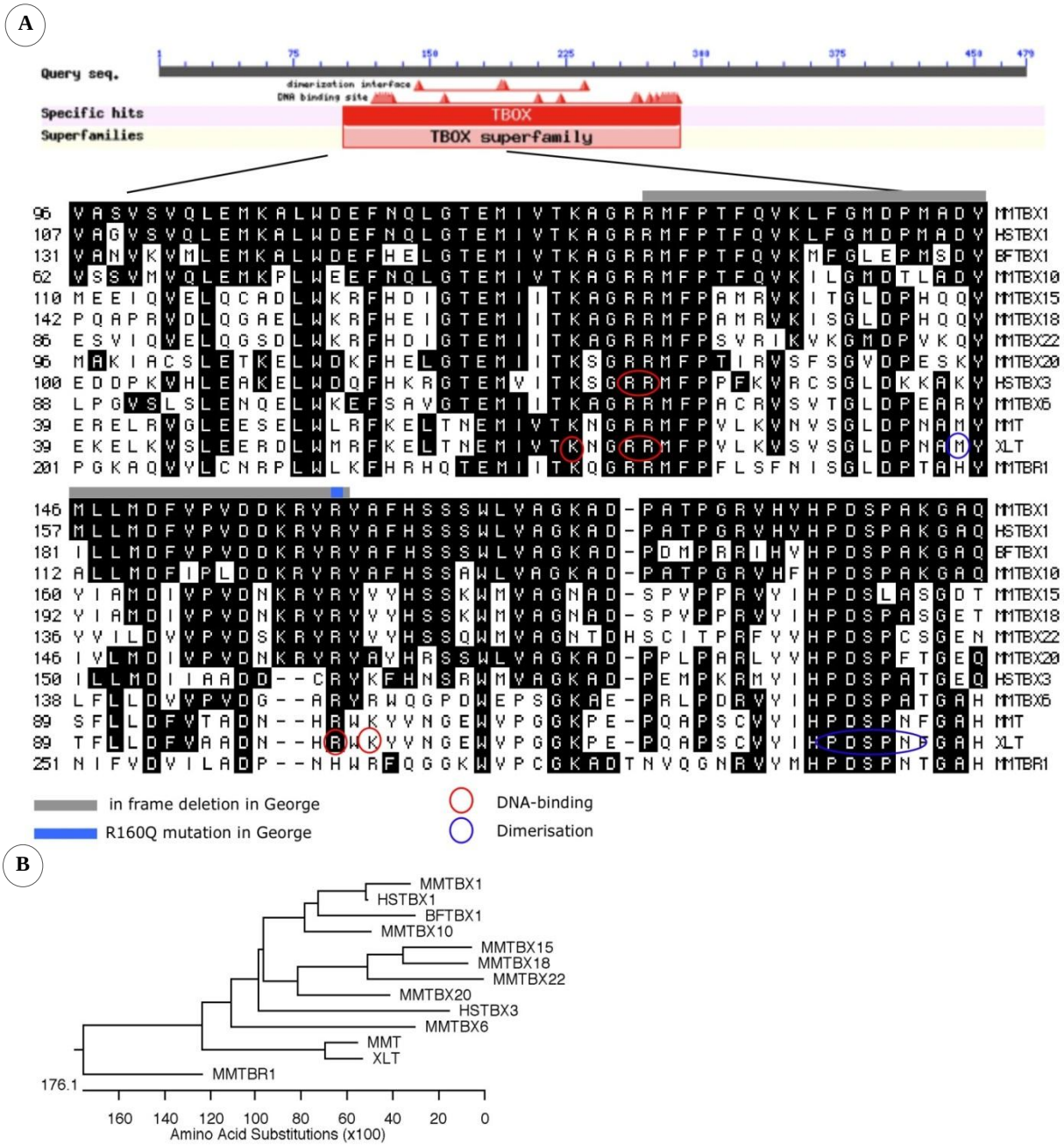

Figure 16. A) Alignement of the DNA-binding domain (T-box) of the members of the T-box superfamily. MM = *Mus musculus*; HS = *Homo sapiens*; BF = *Branchiostoma floridae* and XL = *Xenopus laevis*. The *George* mutation effects proper mRNA splicing by deleting exon 3 in frame. **B)** Phylogenic tree of the T-box superfamily**.**

Since the mutation was located in the consensus splicing donor recognition site at the end of exon 3, it was hypothesized that it could also affect the correct splicing of the *Tbx1* mRNA. We showed by RT-PCR that the mutation was responsible for the skipping of the *Tbx1* exon 3 which coresponds to the deletion of one fifth of the T-box domain. As the T-box domain is highly conserved in all T-box proteins and is responsible for DNA binding as well as TBX1 dimerization, the George mutation could considerably affect the function of TBX1.

4.3.1 The transactivation capacity of TBX1 was reduced by the R160Q mutation but was not affected by the loss of 25% of the T-box domain

Through luciferase assays it was shown that the R160Q amino acid substitution reduced the transactivation capacity of TBX1 significantly. This result was supported by the Biacore protein interaction analysis system which showed that the R160Q point mutation results in a decrease in affinity of TBX1 for its target DNA. It is still unclear whether this increased dissociation constant is due to a weaker interaction between the TBX1 protein and the DNA or whether the mutation affects the stability of the TBX1 dimerization which could also reduce the binding efficiency to the DNA. It is also possible that both of these mechanisms are implicated. However, it is clear that the arginine residue at position 160 is a key residue for *Tbx1* function.

In contrast, the loss of exon 3 did not affect the transactivation capacity of TBX1 to the same extent as the R160Q point mutation. This is a very surprising result as the loss of 25% of the T-box would be expected to result in a much stronger effect on TBX1 function. Unfortunately, the binding affinity of the Ex3del T-box to target DNA could not be assessed using the Surface Plasmon Resonance assay due to the very low stability of mutant protein which we were unable to purify from bacteria. Therefore, the reason for this surprising result could not be determined. However, one possible explanation could be that the dimerization of Ex3del TBX1 is stable enough to allow proper transactivation whereas the R160Q amino acid substitution may render the TBX1 – DNA interaction weaker, resulting in a less stable TBX1 homodimerization. Moreover, it is important to keep in mind that the transactivation experiments were all done using the *Pitx2* promoter. It is possible that other proteins that specifically bind the *Pitx2* promoter are able to stabilize efficiently the Ex3del TBX1 on the DNA. Therefore, if this experiment was repeated on another target promoter, the loss of 25% of the T-BOX could have a different effect on the transactivation capacity of TBX1.

4.3.2 The George phenotype is due to a loss of TBX1 expression

In order to assess the effect of the George mutation on TBX1 protein expression in embryonic tissue, a western blot was performed. This failed to detect any of the predicted mutant forms. Whereas this finding explains the George phenotype, there is the possibility that the proteins are expressed but are below detection level. This hypothesis is supported

by the observation that both forms, the R160Q and the Ex3del TBX1 variants could be expressed in HEK293T cells albeit from a strong CMV promoter. The fact that the Ex3del was expressed but could not be purified from bacteria suggests that this mutation destabilizes the protein which then forms non-functional aggregates. The *George* allele can therefore be defined as a strong hypomorph or as a null allele.

These results indicate that in the mutant, TBX1 proteins are either not or poorly expressed in embryos. In addition, Surface Plasmon Resonance assays suggest that even if there was a residual expression of mutant R160Q TBX1 protein, it would have lower binding affinity to the DNA. Apart from being necessary for the interaction between TBX1 and DNA, the R160 residue, could also be involved in the interaction of TBX1 with other proteins.

CHAPTER 5

Protein interaction network surrounding TBX1

5.1 Rationale to investigate the Protein interaction network surrounding TBX1

Protein-protein interactions (PPIs) are crucial for all biological processes. Therefore, the understanding of PPI networks provides many new insights into protein function and its position in specific pathways. To date, the protein interaction network surrounding TBX1 is poorly characterized and its identification would allow for better understanding of the mechanisms through which the *Tbx1* genotype is linked to the DiGeorge phenotype and explain variable penetrance. The study of the effect of specific point mutations on the physical interaction of TBX1 with the DNA and/or binding partners may provide key answers to this question.

5.2 Results

5.2.1 George affects TBX1 interaction with certain putative interactors

To study the protein interaction network surrounding TBX1 and at the same time determine the effect of the loss of exon 3 on these interactions, several putative TBX1 interactors were selected. Of particular interest were GATA4[149] and PTDSR (also called JMJD6)[150] as these proteins are known to be involved in heart development. NKX2.5[151] and SMAD1[79] were also included in the experiment as they have previously been shown to interact with wild-type TBX1. It has previously been reported that chromatin modification enzymes interact with TBX2[124], another T-box protein, and it was therefore decided to test the interaction between TBX1 and RBBP5 and PTDSR. Finally, SMARCAD1 was selected as it had been pulled-down as a TBX1 binding protein by Dr. R. Kelly's lab (personal communication). All these interactions were studied by performing Protein Complementation assays. This technique allows the detection of protein-protein interactions in cell-based assays by measuring the luminescence resulting from the reconstitution of a fully functional luciferase protein from its two halves if the two proteins of interest interact. In this experiment TBX1 was fused to the first half of renilla luciferase whereas candidate interactors were fused to the second half of renilla luciferase and luminescence was measured after cotrasfecting the two constructs into HEK293T cells (Figure 17).

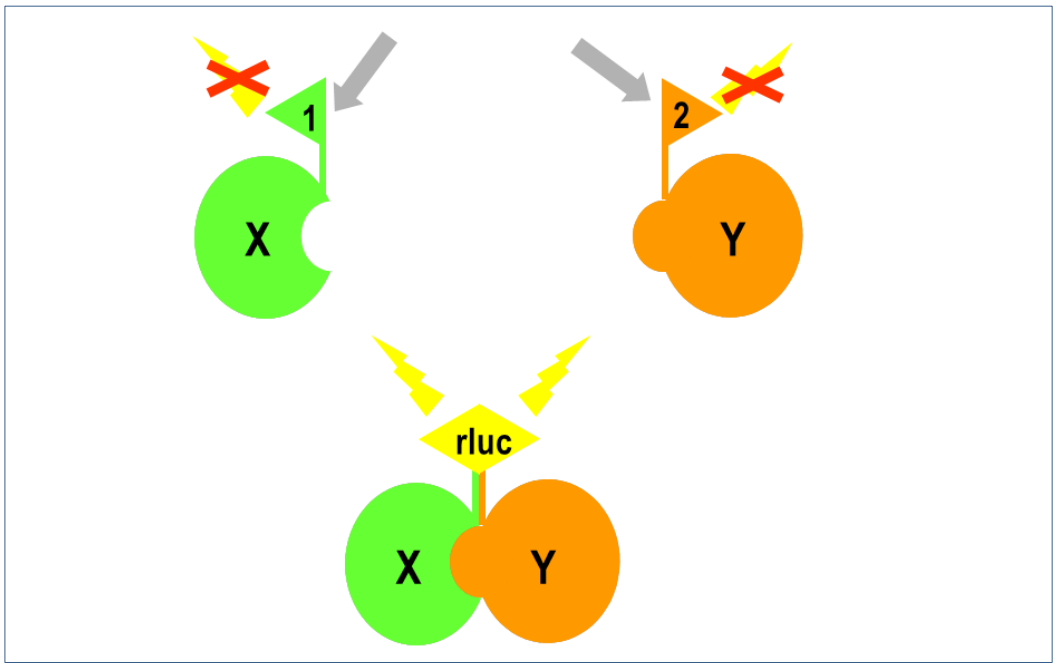

Figure 17. Schematic representation of the Protein Complementation Assays (PCA) to study the interactions between proteins in vitro.

The interaction affinity of the predicted R160Q variant was also examined in these assays. Results showed that wild-type TBX1 homodimerises (Figure 18A), and interacts with transcription factors RBBP5, GATA4, PTDSR and SMARCAD1. Whereas the TBX1-GATA4 interaction was not affected by the R160Q mutation, it was reduced by about 45% by the loss of exon3. The R160Q mutation affected the TBX1-SMARCAD1 interaction by reducing it by 40% and the Ex3del reduced it by 70% (Figure 18B). The known TBX1-NKX2.5 interaction was reduced by 20% by the R160Q mutation and by 55% by the Ex3del. Both mutations reduced the TBX1-SMAD1 interaction by 30% (Figure 18C). The interaction between TBX1 and RBBP5 was significantly reduced by 55% by the R to Q

substitution and by as much as 70% by the loss of exon 3. Finally, the R160Q mutation and the exon 3 deletion reduced the TBX1-PTDSR interaction by 30% and 88% respectively (Figure 18D).

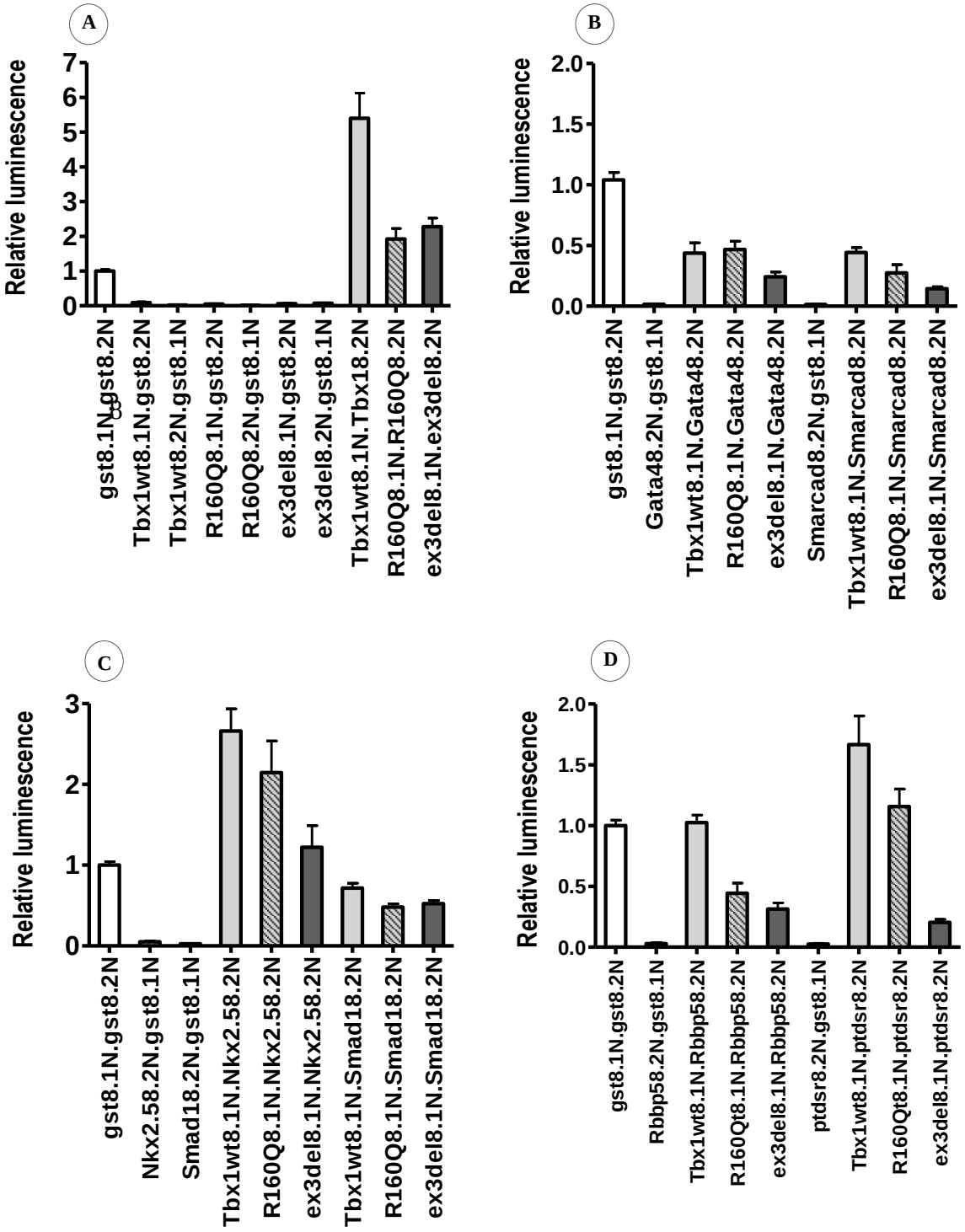

Figure 18. Protein Complementation assay results showing **A)** TBX1 dimerization, **B)** interaction between TBX1 and GATA4 and SMARCAD1, **C)** interaction between TBX1 and NKX2.5 and SMAD1, **D)** interaction between TBX1 and RBBP5 and PTDSR. Luminescence readings and standard error of the mean are indicated. Readings were normalised with LacZ and are standardized against GST-GST dimerization readings (=1).

In summary, the loss of exon 3 reduced all of these interactions and R160Q affected all of the above interactions, except for the TBX1-GATA4 interaction, but to a lesser degree. Therefore, the loss of exon 3 as well as the R160Q point mutation both result in at least the partial disruption of the TBX1 protein interaction network.

Two of these interactions, the homodimerization of wild-type TBX1 and the TBX1-PTDSR interactions, have been confirmed using a second cell-based assay called LUMIER (Figure 19).

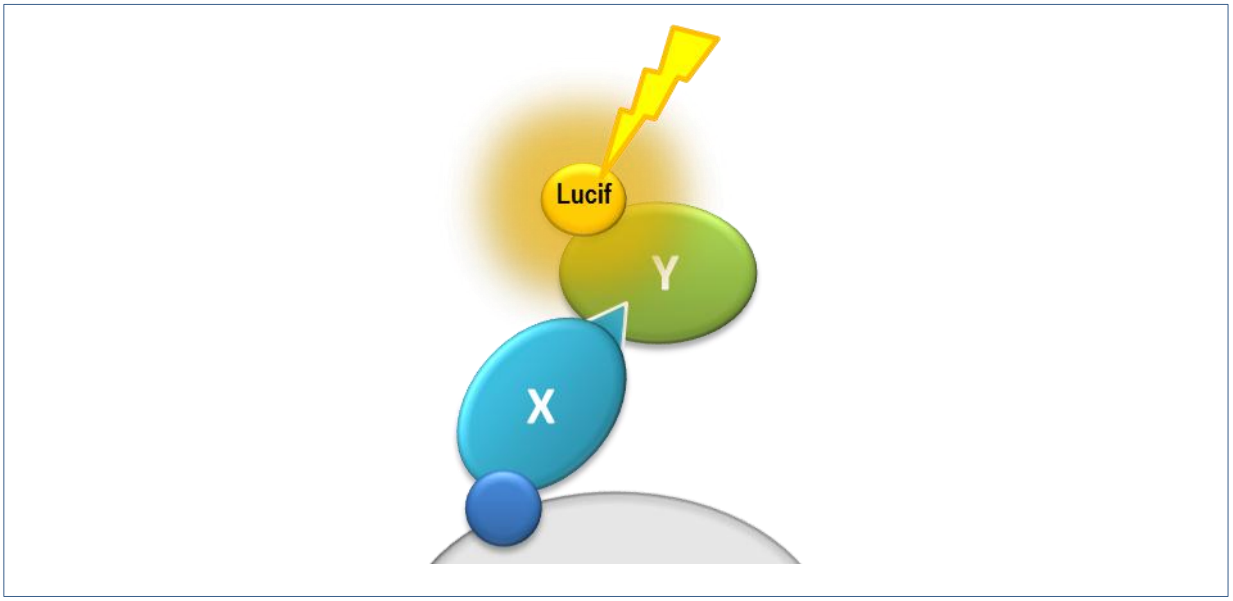

Figure 19. Schematic representation of LUMIER assay.

This assay involves co-immunoprecipitation of the two proteins of interest followed by luminescence-based detection. In this experiment, one of the proteins was his-tagged, allowing it to be recovered the using Cobalt-coated beads, whereas the potential interactor was fused to renilla luciferase, which would allow for the detection of a luminescence

signal if the proteins interacted. Results obtained from this assay confirmed the physical interaction of TBX1 and PTDSR as well as the homodimerization of TBX1 (Figure 20).

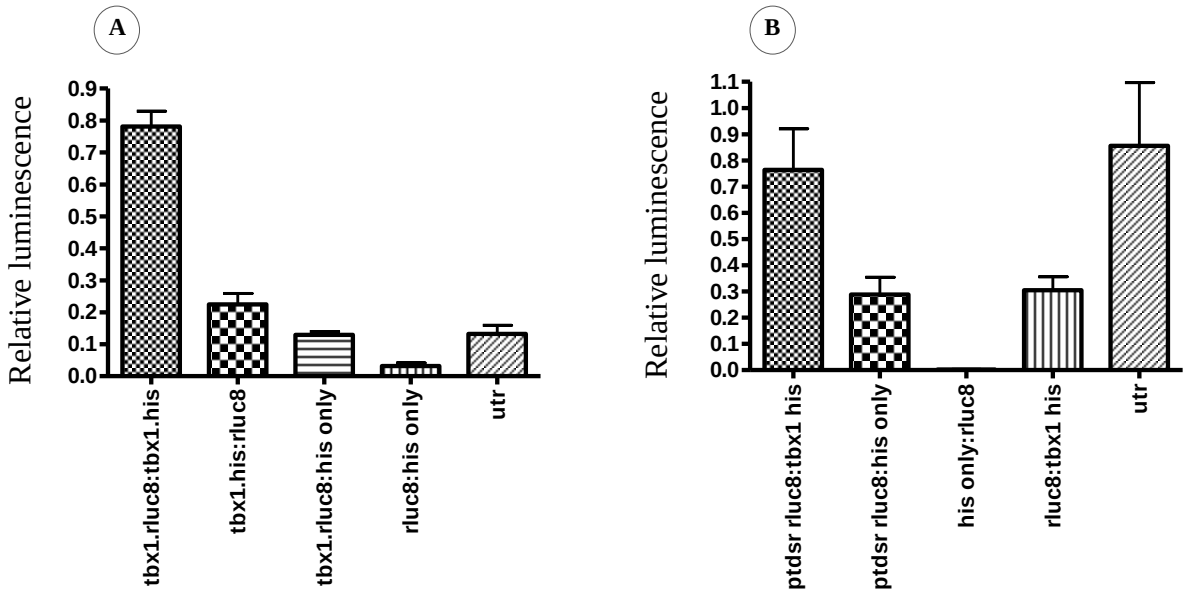

Figure 20. Lumier results showing A) TBX1 homodimerisation and B) interaction between TBX1 and PTDSR. Luminescence readings and standard error of mean are indicated. Results were normalised with LacZ. Negative controls for baseline luminescence and non-specific binding are shown. Utr: untransfected cells.

All the interactions have been measured in "luminescence" and it is difficult to say anything about strengths or affinity of the interaction as luminescence may vary depending on the effect of the renilla fusion on the folding of the proteins of interest. This issue will be addressed more in detail in the discussion.

5.2.2 PTDSR decreases the transactivation capacity of TBX1

In order to understand the functional significance of the TBX1-PTDSR interaction, a luciferase assay with the TBX1 responsive 0.9Pitx2-fluc reporter containing two head-to-head palindromic T-box binding sites (T-half sites) was carried out in HEK293T cells. A constant amount of 20ng of wild-type *TBX1* and increasing amounts of *Ptdsr*, ranging from 0 ng to 20 ng, were cotransfected with the 0.9 *Pitx2*-fluc reporter and luminescence was measured after starving the transfected cells for 12h. Results showed that the transactivation capacity of TBX1 decreased gradually with increasing amounts of *Ptdsr*. Luminescence got reduced by 25% between 0ng and 20ng *Ptdsr* (Figure 21).

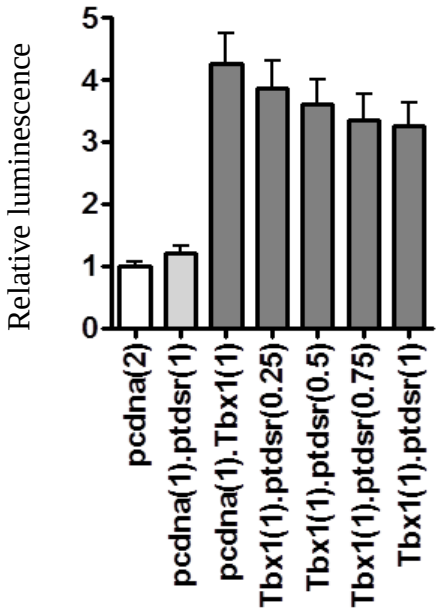

Figure 21. Luciferase assay measuring TBX1 transactivation capacity with different amounts of PTDSR. Luminescence readings and standard error of the mean are indicated. Results are normalised with LacZ and standardised against empty pcdna3 vector (=1).

5.3 Discussion

5.3.1 Importance of understanding the mechanism linking TBX1 genotype and DiGeorge Syndrome phenotype

Whereas the involvement of *TBX1* in heart development and DGS has been know for quite some time, the mechanism through which this happens is far from fully understood. One reason for this lack of knowledge is linked to the limited information available on the protein interaction network surrounding TBX1. Not only would this information allow us to understand the pathogeneis of DGS better, but it could also provide a mechanism why congenital heart malformations have a variable penetrance in DGS as mutations in these genes could potentially reduce the buffering of *TBX1* mutations. Moreover, it will give us a better insight into the position and role of *TBX1* in key developmental pathways which could ultimately lead to the identification of potential preventive methods for cardiac disease.

5.3.2 Identification of novel TBX1 interactors using cell-based assays

In order to understand the network sourronding TBx1, cell-based assays were used to identify new interactors. The decision to use PCA assays was founded on the fact that this technique allows us to asses the interaction between two proteins using human cells and said interaction could be effectively and quickly assessed by measuring luminescence.

These were two significant advantages that could not be found in the split-ubiquitin membrane yeast two-hybrid system. In that system, not only would the interactions be assessed in a distant organism, but the process would have been significantly more time-consuming. However, it is important to note that none of the assays above allow the quantification of the strenght of the interaction mainly because of the dynamic nature of the physical interaction between proteins. In addition to already known interactions between TBX1, NKX2.5 and SMAD1, several new interactions were revealed in this study. The finding of a physical interaction between TBX1 and the transcription factor GATA4 could provide an additional mechanism through which TBX1 is involved in heart development. This research has also allowed the identification of the physical interaction between TBX1 and the DNA modifying enzymes RBBP5, SMARCAD1 and PTDSR. It is therefore possible to hypothesise that acting as a transcriptional activator is not the only function of TBX1 and these results could indicate a potential role of TBX1 in chromatin modification. In order to investigate this further, the physical interaction needs to be confirmed by using an alternative technique, such as Immunoprecipitation or LUMIER assay, and the functional significance of these interactions assessed through transactivation assays and siRNA-mediated knock-down experiments. A further key experiment to characterize these interactions would be to map the domains that physically inetract in both proteins. This could be done by using serial deletions and truncations of the different protein domains in PCA. However, it will be necessary to perform in vivo experiments in order to get a better insight into the biological role of these interactions. The first step would be to investiagte whether there is a genetic interaction between TBX1 and the

potential interactor by using loss of function alleles and crossing them to each other in order to assess the phenotype of the embryos. If there is a genetic interaction between the two proteins, the embryonic malformations of the embryos will be more severe and/or more penetrant than in each of the parents. Alternatively, it could also give rise to a completely new phenotype which is not seen in the single mutants.

5.3.3 Characterization of the TBX1-PTDSR interaction

This thesis also presents the first characterization of the interaction between TBX1 and PTDSR. The study of this interaction was prioritized due to their overlapping phenotype and function: PTDSR and TBX1 are both involved in blood vessel and heart development, and the *Ptdsr* knock out mouse has an overlapping phenotype with the *Tbx1* knock-out mouse, including embryonic lethality, cardiovascular, immune system and craniofacial abnormalities[152]. In addition, *Ptdsr* is known to be involved in cell differentiation, regulation of transcription, chromatin modification, and oxydoreduction[153], which are all processes in which *Tbx1* has an established or potential role.

In addition to PCA, LUMIER assays were performed to confirm the physical interaction between TBX1 and PTDSR. The reason why LUMIER was prefered over Immunoprecipitation is that this new technique is safer as it does not involve radioactivity and should provide quantitative results. Unfortunately, the background signal found in

these experiments was high. The main reason for this is of a technical nature as the protocol involves the washing of magnetic beads by pipetting. This results in the loss of variable amount of beads between the wells. In order to reduce this problem, an automated procedure is currently being optimised in our lab. Another problematic factor could be the affinity of the protein tags (HIS, rluc8) used in this experiment for the magnetic beads. Whereas the presence of the rluc tag is a necessity for the interaction detection, it would be worthwile to substitute the HIS tag with an alternate tag such as flag which might have a lower intrinsic binding affinity for the beads.

Transactivation assays showed that PTDSR could decrease the transactivation capacity of TBX1 on a *Pitx2* reporter. However, the effect was minor. One possible explanation could be that the amount of TBX1 obtained by overexpression is in excess. Thus, any amount of PTDSR can only have a minimal effect on the transactivation capacity of TBX1. Another way to adress this question has been to look at the effect of depleting the endogenous PTDSR from cells and the subsequent ability of TBX1 to transactivate the *Pitx2* promoter. Unfortunately, no conclusions could be drawn from this experiment as the results from three separate repeats were not reproducible. This was mainly due to technical difficulties and cell toxicity associated with the *Ptdsr* siRNA and *TBX1* plasmid cotransfection reagents. An additional issue with this experiment is that *TBX1* is probably expressed in such high levels that it is overriding any inhibition that PTDSR may have been able to exercise. Moreover, the endogenous expression of *Ptdsr* in HEK293T cells might be too low to see an effect. In order to overcome these problems, future experiments should concentrate on using an alternative cell type, such as HeLa cells, which could provide a

higher baseline expression of endogenous *Ptdsr*[154,155]. In these conditions knocking down *Ptdsr* by siRNA has a higher chance to result in any detectable effect on TBX1 transactivation capacity. However, it is possible that the effect of PTDSR on the transactivation capacity of TBX1 is not significant especially not in these artificial conditions with *TBX1* overexpression. In vivo, where *TBX1* is expressed at lower levels, PTDSR may have a detectable inhibitory effect.

Even considering these technical issues associated with the discussed experiments, it would be of greatest interest to pursue this research direction further in order to properly characterize the functional significance of the physical interaction between TBX1 and a chromatin modifying protein. Eventually, these results could potentially show a completely unexpected role of *Tbx1* in biological processes which could open up a whole new research area.

5.3.4 The R160Q point mutation and the Ex3del do affect the interaction of TBX1 with other proteins

Another question that was addressed in this thesis was the effect of the R160Q amino acid substitution and the effect of the loss of the 3rd exon on the interaction of TBX1 with other proteins. The physical interaction between these variants and the interactors was assessed using PCA assay. Results showed that the Arginine residue at position 160 was involved directly or indirectly in TBX1 dimerization. Crystalization of the T-box showed that due to its position close to the DNA it is very likely that this arginine residue is involved in the binding of TBX1 to DNA and that the weakening of this interaction could negatively affect the dimerization between two TBX1 proteins[156]. The results obtained using the Biacore system support this hypothesis. Similarly, the interactions between TBX1 and SMAD1, SMARCAD1, RBBP5 and PTDSR were significantly reduced by the R160Q substitution. One explanation for these results is that the arginine is a key residue implicated directly in the physical interaction of TBX1 and these proteins. Another possibility is, again, that this point mutation affects the stability of the dimerization and binding of TBX1 to the DNA which consequently does not provide a stable enough base for other proteins to bind to the transcriptional activation complex.

The loss of 25% of the T-box domain through the deletion of exon 3 appears to decrease the dimerization capacity of TBX1. However, whereas this observation could be explained by the same mechanisms discussed for the R160Q variant, it is also possible that this

deletion results in a major change in the 3D structure of the protein which could result in an increased physical distance between the two renilla halves, thus affecting the luminescence reading. It is important to keep this aspect in mind also when comparing and interpreting the results for other protein interactions. All interactions between TBX1 and other proteins that were tested were affected by the the loss of exon 3. On the basis of these results, it is not possible to know the underlying reason for this observation which could be due to the loss of stability of TBX1 itself, or due to the requirement of exon 3 in the physical interaction between TBX1 and other proteins. Alternatively, the changes in the TBX1 protein folding resulting from the deletion of exon 3 might alter the recognition site for the interactors. The understanding of how mutations in TBX1 can affect its interaction capacity with other proteins could provide important information on the pathogenic mechanism underlying DiGeorge syndrome as well as providing a better insight into the role of different functional domains and residues of TBX1.

CHAPTER 6

Final Discussion and Conclusion

In the study of diseases, the most interesting and rarely answered question is: why does the same mutation not always cause the same phenotype. This applies particularly to families where a child is diagnosed with a syndrome linked to a defect in a particular gene and after genetically testing the normal parents it appears that one of them carries the exact same mutation. As it has been discussed in the introduction, there are two principal factors responsible for this phenomenon: 1) environmental variation and 2) presence of additional variants/mutations somewhere else in the genome.

In this thesis, a model of DGS has been studied and potential mechanisms for buffering of *Tbx1* deficiency have been addressed. It was shown that preconceptional maternal high fat diet does not affect the penetrance and severity of cardiac malformations of the offspring in our DG murine model (*Df1*). So although environmental variation clearly plays a role in the development of CHD, I propose that rather than affecting heart morphogenesis in general, it interacts with specific genetic factors such as *Cited2*.

Moreover, a *Tbx1* allele which harbours a point mutation and phenocopies the complete DGS phenotype (*George*) has been studied, and it was shown that an arginine to glutamine

amino acid substitution at the position 160 decreased the transactivation capacity of TBX1 dramatically at the Pitx2 promoter, whereas the loss of 25% of the T-box did not have any significant effect. Therefore, this work further supports the idea that *Tbx1* mutations are the major causal factor in DGS.

New potential TBX1 interactors have been identified using luminescence-based assays, and it was shown that the R160Q amino acid substitution as well as the Ex3del affect these interactions. These results imply that mutations in *TBX1* can affect its function at different levels and, as the DG phenotype is known to be TBX1 dosage dependent, it is probable that the penetrance and severity of the phenotype is also a function of the integrity of the protein interaction network surrounding TBX1.

The ultimate goal of the study of the mechanisms responsible for a disease is to identify potential factors or therapeutic targets for prevention and treatment. In order to achieve this aim, it is of fundamental importance to understand all the actors implicated in the development of the disease. This applies particularly to the study of CHD as heart morphogenesis is a very complex process involving a large number of genes and their associated genetic pathways. The study of the effect of the environment on cardiac development, combined with human epidemiological data, provides vital information on how dietary changes could protect the embryo from developing malformations even if they carry a specific genetic variation. In addition to the well-known example of folic acid, studies in rats have shown that the supplementation of the maternal diet with specific vitamins and antioxidants has a protective effect on embryonic development[39,40]. There is

therefore much hope that future studies will uncover new ways to prevent CHD through dietary changes in pregnant women.

By studying how causative mutations affect the function and the interaction of the proteins in their network, scientists will be able to uncover the mechanisms underlying the perturbation of proper embryogenesis. Thanks to the rapidly evolving scientific technology, in particular high throughput drug screening methods, it will be possible to "complement" and rebalance the perturbed genetic pathways.

The hope of a better world where CHD, which has often a devastating effect on quality of life of the affected children and adults, can be prevented and also cured was the thought that motivated this research…and will hopefully motivate many other scientists to continue to explore the genetic and environmental basis of CHD.

Abbreviations

AoA	Aortic Arch
ASD	Atrial Septal Defect
CAT	Common Arterial Trunk
CD	Control Diet
CHD	Congenital Heart Disease
DA	Ductus Arteriosus
DGS	DiGeorge Syndrome
ENU	Ethylnitrosourea
HFD	High-Fat Diet
IAA	Interrupted Aortic Arch
MRI	Magnetic Resonance Imaging
OFT	Outflow Tract
RAA	Right-sided Aortic Arch
TOF	Tetralogy of Fallot
VSD	Ventricular Septal Defect
VR	Vascular Ring

Table of Figures

Acknowledgements

I would like to express my deep gratitude to my two supervisors, Professor Shoumo Bhattacharya and Professor Hugh Watkins, who have guided, supported and motivated me throughout this work. Thank you Shoumo for your time and your enthusiasm and for giving me the opportunity to learn from you. Above all, thank you for teaching me not to believe anything in science until it has been demonstrated and proven. Hugh, thank you for your encouragement, your valuable advice and the stimulating discussions, which have allowed me to get a deeper understanding of Genetics.

Thank you to all the present and former Bhattacharya and Davies Lab members: Akshay Kumar Ahuja, Angela Franklyn, Anna Michell, Anuja Neve, Ayman Al Haj Zen, Ben Davies, Bradley Joyce, Carol Broadbent, Catherine Cosgrove, Chris Preece, Daniel Andrews, Daniel Biggs, Dorota Szumska, Hamid Dolatshad, Hanneng Zhu, Jamie Bentham, Jose Braganca, Karen Sogaard, Matthew Benson, Michal Bilski, Milena Cioroch, Simon Bamforth and Wei Ji for your help and for the many discussions about the work presented in this thesis. It was a fantastic and enriching experience to share the last 4 years with such great people. Thank you.

Special thanks goes to my dearest friend Sheny Chen. Thank you Sheny for always being there for me. Your knowledge is truly amazing and I learned so much from you about science and life in general. Everything sounded so much easier after talking to you. Above all, I wish to thank you for being such a fabulous and caring friend which made my PhD a fantastic journey. I will always treasure the memory of our time spent together and our late afternoon conversations. I will miss you so much.

I am very grateful to Kamel El-Omari for his help, patience and generosity. I thoroughly enjoyed working with you and learned a lot. Thank you also to Rosa Morra for her precious help with the Surface Plasmon Resonance experiment.

I am indebted to Jan Duff, Lynn Clee and Kathryn Smith for their kindness and precious help with administrative duties. Thank you to James Brown and Phil Townsend for always being ready to help and making my life so much easier.

I would like to thank the British Heart Foundation for funding this work.

I am immensely grateful to my parents, Nadine and Alain, and to my sister Stéphanie for their unconditional love and support. Thank you for transmitting your passion for science and for letting me follow my dreams.

Most importantly I would like to thank my beloved husband Claudio Screpanti and my little daughter Amélie who joined us while I was writing this thesis. You are my constant source of love, hope and inspiration. Thank you Claudio for your endless love, patience and support. Thank you for helping me focus and for reminding me to look at the global picture instead of obsessing over details. This thesis would not have been possible without you. Thank you for believing in me and for being who you are. Living by your side is a dream. Amélie, you brought more meaning to my life than you will ever know. Your smile fills my heart with happiness.

BIBLIOGRAPHY

1 Schultheiss, T. M., Xydas, S., Lassar, A.B. Induction of avian cardiac myogenesis by anterior endoderm. *Development* **121**, 4203-4214 (1995).

2 Brand, T. Heart development: molecular insights into cardiac specification and early morphogenesis. *Dev Biol.* **258**, 1-19 (2003).

3 Cripps, R. M., Olson, E.N. Control of cardiac development by an evolutionarily conserved transcriptional network. *Dev Biol.* **246**, 14-28 (2002).

4 Xu, H., Baldini, A. Genetic pathways to mammalian heart development: Recent progress from manipulation of the mouse genome. *Semin Cell Dev Biol.* **18**, 77-83 (2007).

5 Srivastava, D., Olson, E.N. A genetic blueprint for cardiac development. *Nature* **407**, 221-226 (2000).

6 Capdevila, J., Vogan, K.J., Tabin, C.J., Izpisua Belmonte, J.C. Mechanisms of left-right determination in vertebrates. *Cell* **101**, 9-21 (2000).

7 Brown, C. B., Boyer, A.s., Runyan, R.B., Barnett, J.V. Requirement of type III TGF-beta receptor for endocardial cell transformation in the heart. *Science* **283**, 2080-2082 (1999).

8 Kirby, M. L., Waldo, K.L. Neural crest and cardiovascular patterning. *Circ Res* **77**, 211-215 (1995).

9 Hoffman, J. I., Kaplan, S. The incidence of congenital heart disease. *J Am Coll Cardiol* **39**, 1890-1900 (2002).

10 Vonder Muhll, I., Cumming, G., Gatzoulis, M.A. Risky business: insuring adults with congenital heart disease. *Eur Heart J.* **24**, 1595-1600 (2003).

11 Mitchell, S. C., Korones, S.B., Berendes, H.W. Congenital heart disease in 56,109 births. Incidence and natural history. *Circulation* **43**, 323-332 (1971).

12 Wren, C., O'Sullivan, J.J. Survival with congenital heart disease and need for follow up in adult life. *Heart* **85**, 438-443 (2001).

13 Miller, S. P., McQuillen, P.S., Hamrick, S., Xu, D., Glidden, D.V., Charlton, N., Karl, T., Azakie, A., Ferriero, D.M., Barkovich, A.J., Vigneron, D.B. Abnormal brain development in newborns with congenital heart disease. *N Engl J Med.* **357**, 1928-1938 (2007).

14 Ferencz, C., Boughman, J.A., Neill, C.A., Brenne, J.I., Perry, L.W. Congenital cardiovascular malformations: questions on inheritance. Baltimore-Washington Infant study group. *J Am Coll Cardiol* **14**, 756-763 (1989).

15 Bentham, J., Bhattacharya, S. Genetic mechanisms controlling cardiovascular development. *Ann N Y Acad Sci.* **1123**, 10-19 (2008).

16 Bruneau, B. G. The developmental genetics of congenital heart disease. *Nature* **451**, 943-948 (2008).

17 Basson, C. T., Bachinsky, D.R., Lin, R.C., Levi, T., Elkins, J.A., Soults, J., Grayzel, D., Kroumpouzou, E., Traill, T.A., Leblanc-Straceski, J., Renault, B., Kucherlapati, R., Seidman, J.G., Seidman, C.E. Mutations in human TBX5 cause limb and cardiac malformation in Holt-Oram syndrome. *Nat Genet.* **15**, 30-35 (1997).

18 Bruneau, B. G., Nemer, G., Schmitt, J.P., Charron, F., Robitaille, L., Caron, S., Conner, D.A., Gessler, M., Nemer, M., Seidman, C.E., Seidman, J.G. A murine model of Holt-Oram syndrome defines roles of the T-box transcription factor Tbx5 in cardiogenesis and disease. *Cell* **106**, 709-721 (2001).

19 Schott, J. J., Benson, D.W., Basson, C.T., Pease, W., Silberbach, G.M., Moak, J.P., Maron, B.J., Seidman, C.E., Seidman, J.G. Congenital heart disease caused by mutations in the transcription factor NKX2-5. *Science* **281**, 108-111 (1998).

20 Benson, D. W., Silberbach, G.M., Kavanaugh-McHugh, A., Cottrill, C., Zhang, Y., Riggs, S., Smalls, O., Johnson, M.C., Watson, M.S., Seidman, J.G., Seidman, C.E. Mutations in the cardiac transcription factor NKX2.5 affect diverse cardiac developmental pathways. *J Clin Invest.* **104**, 1567-1573 (1999).

21 Garg, V., Kathiriya, I.S., Barnes, R., Schluterman, M.K., King, I.N., Butler, C.A., Rothrock, C.R., Eapen, R.S., Hirayama-Yamada, K., Joo, K., Matsuoka, R., Cohen, J.C., Srivastava, D. GATA4 mutations cause human congenital heart defects and reveal an interaction with TBX5. *Nature* **424**, 443-447 (2003).

22 Lindsay, E. A., Vitelli, F., Su, H., Morishima, M., Huynh, T., Pramparo, T., Jurecic, V., Ogunrinu, G., Sutherland, H.F., Scambler, P., Bradley, A., Baldini, A. *Tbx1* haploinsufficiency in the DiGeorge syndrome region causes aortic arch defects in mice. *Nature* **410**, 97-101 (2001).

23 Merscher, S., Funke, B., Epstein, J.A., Heyer, J., Puech, A., Lu, M.M., Xavier, R.J., Demay, M.B., Russel, R.G., Factor, S., Tokooya, K., St. Jore, B., Lopez, M., Pandita, R.K., Lia, M., Carrion, D., Xu, H., Schorle, H., Kobler, J.B., Scambler, P., Wynshaw-Boris, A., Skoultchi, A.I., Morrow, B.E., Kucherlapati, R. *TBX1* is responsible for cardiovascular defects in Velo-Cardio-Facial/DiGeorge syndrome. *Cell* **104**, 619-629 (2001).

24 Yagi, H., Furutani, Y., Hamada, H., Sasaki, T., Asakawa, S., Minoshima, S., Ichida, F., Joo, K., Kimura, M., Imamura, S., Kamatani, N., Momma, K., Takao, A., Nakazawa, M., Shimizu, N., Matsuoka, R. Role of TBX1 in human del22q11.2 syndrome. *Lancet* **362**, 1366-1373 (2003).

25 Guris, D. L., Duester, G., Papaioannou, V.E., Imamoto, A. Dose-dependent interaction of Tbx1 and Crkl and locally aberrant RA signaling in a model of del22q11 syndrome. *Dev Cell.* **10**, 81-92 (2006).

26 Moon, A. M., Guris, D.L., Seo, J.H., Li, L., Hammond, J., Talbot, A., Imamoto, A. Crkl deficiency disrupts Fgf8 signaling in a mouse model of 22q11 deletion syndrome. *Dev Cell.* **10**, 71-80 (2006).

27 Al-Baradie, R., Yamada, K., St. Hilaire, C., Chan, W.M., Andrews, C., McIntosh, N., Nakano, M., Martonyi, E.J., Raymond, W.R., Okumura, S., Okihiro, M.M., Engle, E.C. Duane radial ray syndrome (Okihiro syndrome) maps to 20q13 and results from mutations in SALL4, a new member of the SAL family. *Am J Hum Genet.* **71**, 1195-1199 (2002).

28 Kohlhase, J., Heinrich, M., Schubert, L., Liebers, M., Kispert, A., Laccone, F., Turnpenny, P., Winter, R.M., Reardon, W. Okihiro syndrome is caused by SALL4 mutations. *Hum Mol Genet.* **11**, 2979-2987 (2002).

29 Koshiba-Takeuchi, K., Takeuchi, J.K., Arruda, E.P, Kathiriya, I.S., Mo, R., Hui, C.C., Srivastava, D., Bruneau, B.G. Cooperative and antagonistic interactions between Sall4 and Tbx5 pattern the mouse limb and heart. *Nat Genet.* **38**, 175-183 (2006).

30 Kirk, E. P., Sunde, M., Costa, M.W., Rankin, S.A., Wolstein, O., Castro, M.L., Butler, T.L., Hyun, C., Guo, G., Otway, R., Mackay, J.P., Waddell, L.B., Cole, A.D., Hayward, C., Keogh, A., Macdonald, P., Griffiths, L., Fatkin, D., Scholler, G.F., Zorn, A.M., Feneley, M.P., Winlaw, D.S., Harvey, R.P. Mutations in cardiac T-box factor gene TBX20 are associated with diverse cardiac pathologies, including defects of septation and valvulogenesis and cardiomyopathy. *Am J Hum Genet.* **81**, 280-291 (2007).

31 Hiroi, Y., Kudoh, S., Monzen, K., Ikeda, Y., Yazaki, Y., Nagai, R., Komuro, I. Tbx5 associates with Nkx2-5 and synergistically promotes cardiomyocyte differentiation. *Nat Genet.* **28**, 276-280 (2001).

32 Srivastava, D. Making or breaking the heart: from lineage determination to morphogenesis. *Cell* **126**, 1037-1048 (2006).

33 Lickert, H., Takeuchi, J.K., Von Both, I., Walls, J.R., McAuliffe, F., Adamson, S.L., Henkelman, R.M., Wrana, J.L., Rossant, J., Bruneau, B.G. Baf60c is essential for function of BAF chromatin remodelling complexes in heart development. *Nature* **432**, 107-112 (2004).

34 Gottlieb, P. D., Pierce, S.A., Sims, R.J., Yamagishi, H., Weihe, E.K., Harriss, J.V., Maika, S.D., Kuziel, W.A., King, H.L., Olson, E.N., Nakagawa, O., Srivastava, D. Bop encodes a muscle-restricted protein containing MYND and SET domains and is essential for cardiac differentiation and morphogenesis. *Nat Genet.* **31**, 25-32 (2002).

35 Jenkins, K. J., Correa, A., Feinstein, J.A., Botto, L., Britt, A.E., Daniels, S.R., Elixson, M., Warnes, C.A., Webb, C.L., American Heart Association Council on Cardiovascular Disease in the Young. Noninherited risk factors and congenital cardiovasculoar defects: current knowledge: a scientific statement from the American Heart Association Council on Cardiovascular Disease in the Young: endorsed by the American Academy of Pediatrics. *Circulation* **115**, 2995-3014 (2007).

36 Mikhail, L. N., Walker, C.K., Mittendorf, R. Association between maternal obesity and fetal cardiac malformations in African Americans. *J Natl Med Assoc.* **94**, 695-700 (2002).

37 Watkins, M. L., Rasmussen, S.A., Honein, M.A., Botto, L.D., Moore, C.A. Maternal obesity and risk for birth defects. *Pediatrics* **111**, 1152-1158 (2003).

38 Loeken, M. R. Advances in understanding the molecular causes of diabetes-induces birth defects. *J Soc Gynecol Investig.* **13**, 2-10 (2006).

39 Eriksson, U. J., Siman, C.M. Pregnant diabetic rats fed the antioxydant hydroxytoluene show decreased occurence of malformation in offspring. *Diabetes* **45**, 1497-1502 (1996).

40 Reece, E. A., Wu, Y.K. Prevention of diabetic embryopathy in offspring of diabetic rats with use of a cocktail of deficient substrates and an antioxidant. *Am J Obstet Gynecol* **176**, 790-797 (1997).

41 Salbaum, J. M., Kappen, C. Diabetic embryopathy: a role for the epigenome? *Birth Defects Res A Clin Mol Teratol* **91**, 770-780 (2011).

42 Botto, L. D., Erickson, J.D., Mulinare, J., Lynberg, M.C., Liu, Y. maternal fever, multivitamin use, and selected birth defects: evidence of interaction? *Epidemiology* **13**, 485-488 (2002).

43 Tikkanen, J., Heinonen, O.P. Maternal hyperthermia during pregnancy and cardiovascular malformations in the offspring. *Eur J. Epidemiol* **7**, 628-635 (1991).

44 Edwards, M. J. Apoptosis, the heat shock response, hyperthermia, birth defects, disease and cancer. Where are the common links? *Cell Stress Chaperones* **3**, 213-220 (1998).

45 Loeser, H., Majewski, F. Type and frequency of cardiac defects in embryofetal alcohol syndrome. Report of 16 cases. *Br Heart J.* **39**, 1374-1379 (1977).

46 Samren, E. B., van Duijn, C.M., Christiaens, G.C., Hofman, A., Lindhout, D. Antiepileptic drug regimens and major congenital abnormalities in the offspring. *Ann Neurol* **46**, 739-746 (1999).

47 Zierler, S., Rothman, K.J. Congenital heart disease in relation to maternal use of Bendectin and other drugs in early pregnancy. *N Engl J Med.* **313**, 347-352 (1985).

48 Ericson, A., Kallen, B.A. Nonsteroidal anti-inflammatory drugs inearly pregnancy. *Reprod. Toxicol.* **15**, 371-375 (2001).

49 Ostensen, M. Nonsteroidal anti-inflammatory drugs during pregnancy. *Scand J Rheumatol Suppl* **107**, 128-132 (1998).

50 Czeizel, A. E., Rockenbauer, M., Sorensen, H.T., Olsen, J. The teratogenic risk of trimethoprim-sulfonamides: a population based case-control study. *Reprod. Toxicol.* **15**, 637-646 (2001).

51 Newschaffer, C. J., Cocroft, J., Anderson, C.E., Hauck, W.W., Turner, B.J. Prenatal zidovudine use and congenital anomalies in a medicaid population. *J Acquir Immune Defic Syndr.* **24**, 249-256 (2000).

52 Kallen, K. Maternal smoking, body mass index, and neural tube defects. *Am J Epidemiol* **147**, 1103-1111 (1998).

53 Shaw, G. M., Todoroff, K., Finnell, R.H., Lammer, E.J. Spina bifida phenotypes in infants or feruses of obese mothers. *Teratology* **61**, 376-381 (2000).

54 Shaw, G. M., Velie, E.M., Schaffer, D. Risk of neural tube defects-affected pregnancies among obese women. *JAMA* **275**, 1093-1096 (1996).

55 Waller, D. K., Shaw, G.M., Rasmussen, S.A., Hobbs, C.A., Canfield, M.A., Siega-Riz, A.M., Gallaway, M.S., Correa, A., National Birth Defects Prevention Study. Prepreganancy obesity as a rik factor for structural birth defects. *Arch Pediatr Adolesc Med* **161**, 745-750 (2007).

56 Cedergren, M., Kallen,. B. Maternal obesity and the risk for orofacial clefts in the offspring. *Cleft Palate Craniofac J* **42**, 367-371 (2005).

57 Cedergren, M. I., Selbing, A.J., Kallen, B.A. Risk factors for cardiovascular malformation - a study based on prospectively collected data. *Scand J Work Environ Health* **28**, 12-17 (2002).

58 Watkins, M. L., Botto, L.D. Maternal prepregnancy weight and congenital heart defects in the offspring. *Epidemiology* **11**, 439-446 (2001).

59 Cedergren, M. I., Kallen, B.A. Maternal obesity and infant heart defects. *Obes Res* **11**, 1065-1071 (2003).

60 Carmichael, S. L., Yang, W., Feldkamp, M.L., Munger, R.G., Siega-Riz, A.M., Botto, L.D., Shaw, G., for the National Birth Defects Prevention Study. Reduced risks of neural tube defects and orofacial clefts with higher diet quality. *Arch Pediatr Adolesc Med* (2011).

61 Wolfe, H. M., Sokol, R.J., Martier, S.M., Zador, I.E. Maternal obesity: a potential source of error in sonographic prenatal diagnosis. *Obstet Gynecol* **76**, 339-342 (1990).

62 Botto, L. D., May, K., Fernhoff, P.M., Correa, A., Coleman, K., Rasmussen, S.A., Merritt, R.K., O'Leary, L.A., Wong, L.Y., Elixson, E.M., Mahle, W.T., Campbell, R.M. A population-based study of the 22q11.2 deletion: phenotype, incidence, and contribution to major birth defects in the population. *Pediatrics* **112**, 101-107 (2003).

63 Ryan, A. K., Goodship, J.A., Wilson, D.I., Philip, N., Levy, A., Seidel, H., Schuffenhauer, S., Oechsler, H., Belohradsky, B., Prieur, M., Aurias, A., Raymond, F.L., Clayton-Smith, J., Hatchwell, E., McKeown, C., Beemer, F.A., Dallapiccola, B., Novelli, G., Hurst, J.A., Ignatius, J., Green, A.J., Winter, R.M., Brueton, L., Brondum-Nielsen, K., Scambler, P.J., et al. Spectrum of clinical features associated with interstitial chromosome 22q11 deletions: a European collaborative study. *J Med Genet.* **34**, 798-804 (1997).

64 Dodson, W. E., Alexander, D., Al-Aish, M., De La Cruz, F. The DiGeorge syndrome. *Lancet* **1**, 574-575 (1969).

65 Halford, S., Lindsay, E., Nayudu, M., Carey, A.H., Baldini, A., Scambler, P.J. Low-copy-number repeat sequences flank the DiGeorge/velo-cardio-facial syndrome loci at 22q11. *Hum Mol Genet.* **2**, 191-196 (1993).

66 Edelmann, L., Pandita, R.K., Morrow, B.E. Low-copy repeats mediate the common 3-Mb deletion in patients with velo-cardio-facial syndrome. *Am J Hum Genet.* **64**, 1076-1086 (1999).

67 Edelmann, L., Pandita, R.K., Spiteri, E., Funke, B., Goldberg, R., Palanisamy, N., Chaganti, R.S., Magenis, E., Shprintzen, R.J., Morrow, B.E. A common molecular basis for rearrangement disorders on chromosome 22q11. *Hum Mol Genet.* **8**, 1157-1167 (1999).

68 Shaikh, T. H., Kurahashi, H., Saitta, S.C., O'Hare, A.M., Hu, P., roe, B.A., Driscoll, D.A., McDonald-McGinn, D.M., Zackai, E.H., Budarf, M.L., Emanuel, B.S. Chromosome 22-specific low copy repeats and the 22q11.2 deletion syndrome: genomic organization and deletion endpoint analysis. *Hum Mol Genet.* **9**, 489-501 (2000).

69 Baldini, A. Dissecting contiguous gene defects: *TBX1*. *Curr. Opin. Genet. Dev.* **15**, 279-284 (2005).

70 Kimber, W. L., Hsieh, P., Hirotsune, S., Yuva-Paylor, L., Sutherland, H.F., Chen, A., Ruiz-Lozano, P., Hoogstraten-Miller, S.L., Chien, k.R., paylor, R., Scambler, P.J., Wynshaw-Boris, A. Deletion of 150kb in the minimal DiGeorge/velocardiofacial syndrome critical region in mouse. *Hum Mol Genet.* **8**, 2229-2237 (1999).

71 Lindsay, E. A., Botta, A., Jurecic, V., Carattini-Rivera, S., Cheah, Y.-C., Rosenblatt, H.M., Bradley, A., Baldini, A. Congenital heart disease in mice deficient for the DiGeorge syndrome region. *Nature* **401**, 379-383 (1999).

72 Jerome, L. A., Papaioannou, V.E. Di George syndrome phenotype in mice mutant for the T-box gene, *Tbx1*. *Nat. Genet.* **27**, 286-291 (2001).

73 Zhang, Z., Baldini, A. *In vivo* response to high-resolution variation of Tbx1 mRNA dosage. *Hum. Mol. Genet.* **17**, 150-157 (2008).

74 Roberts, C., Sutherland, H.F., Farmer, H., Kimber, W., Halford, S., Carey, A., Brickman, J.M., Wynshaw-Boris, A., Scambler, P.J. Targeted mutagenesis of the Hira gene results in gastrulation defects and patterning abnormalities of mesoendodermal derivatives prior to early embryonic lethality. *Mol Cell Biol.* **22**, 2318-2328 (2002).

75 Guris, D. L., Fantes, J., Tara, D., Druker, B.J., Imamoto, A. Mice lacking the homologue of the human 22q11.2 gene CRKL phenocopy neurocristopathies of DiGeorge syndrome. *Nat Genet.* **27**, 293-298 (2001).

76 Conrad, M., Jakupoglu, C., Moreno, S.G., Lippl, S., Banjac. A., Schneider, M., Beck, H., Hatzopoulos, A.K., Just, U., Sinowatz, F., Schmahl, W., Chien, K.R., Wurst, W., Bornkamm, G.W., Brielmeier, M. Essential role for mitochondrial thioredoxin reductase in hematopoiesis, heart development, and heart function. *Mol Cell Biol.* **24**, 9414-9423 (2004).

77 Zweier, C., Sticht, H., Aydin-Yaylagul, I., Campbell, C.E., Rauch, A. Human Tbx1 missense mutations cause gain of function resulting in the same phenotype as 22q11.2 deletions. *Am. J. Hum. Genet.* **80**, 510-517 (2007).

78 Paylor, R., Glaser, B., Mupo, A., ataliotis, P., Spencer, C., Sobotka, A., Sparks, C., Choi, C.H., Oghalai, J., Curran, S., Murphy, K.C., Monks, S., Williams, N., O'Donovan, M.C., Owen, M.J., Scambler, P.J., Lindsay, E. Tbx1 haploinsufficiency is linked to behavioral disorders in mice and humans: implications for 22q11 deletion syndrome. *Proc. Natl. Acad. Sci. USA* **103**, 7729-7734 (2006).

79 Fulcoli, F. G., Huynh, T., Scambler, P.J., Baldini, A. Tbx1 regulates the BMP-Smad1 pathway in a transcription independent manner. *PLoS One.* **4**, e6049 (2009).

80 Wang, J., Greene, S.B., Bonilla-Claudio, M., Tao, Y., Zhang, J., Bai, Y., Huang, Z., Black, B.L., Wang, F., Martin, J.F. Bmp signaling regulates myocardial differentiation from

cardiac progenitors through a MicroRNA-mediated mechanism. *Dev. Cell.* **19**, 903-912 (2010).

81 Hu, T., Yamagishi, H., Maeda, J., McAnally, J., Yamagishi, C., Srivastava, D. Tbx1 regulates fibroblast growth factors in the anterior heart field through a reinforcing autoregulatory loop involving forkhead transcription factors. *Development* **131**, 5491-5502 (2004).

82 Xu, H., Morishima, M., Wylie, J.N., Schwartz, R.J., Bruneau, B.G., Lindsay, E.A., Baldini, A. Tbx1 has a dual role in the morphogenesis of the cardiac outflow tract. *Development* **131**, 3217-3227 (2004).

83 Kelly, R. G., Papaioannou, V.E. Visualization of outflow tract development in the absence of Tbx1 using an FgF10 enhancer trap transgene. *Dev Dyn* **236**, 821-828 (2007).

84 Vitelli, F., Taddei, I., Morishima, M., Meyers, E.N., Lindsay, E.A., Baldini, A. A genetic link between *Tbx1* and fibroblast growth factor signaling. *Development* **129**, 4605-4611 (2002).

85 Park, E. J., Ogden, L.A., Talbot, A., Evans, S., Cai, C-L., Black, B.L., Frank, D.U., Moon, A.M. Required, tissue-specific roles for Fgf8 in outflow tract formation and remodeling. *Development* **133**, 2419-2433 (2006).

86 Watanabe, Y., Miyagawa-Tomita, S., Vincent, S.D., Kelly, R.G., Moon, A.M., Buckingham, M.E. Role of mesodermal FGF8 and FGF10 overlaps in the development of the arterial pole of the heart and pharyngeal arch arteries. *Circ Res* **106**, 495-503 (2010).

87 Vitelli, F., Lania, G., Huynh, T., Baldini, A. Partial rescue of the *Tbx1* mutant heart phenotype by *Fgf8*: Genetic evidence of impaired tissue response to *Fgf8*. *J. Mol. Cell. Cardiol.* **49**, 836-840 (2010).

88 Calmont, A., Ivins, S., Van Bueren, K.L., Papangeli, I., Kyriakopoulou, V., Andrews, W.D., Martin, J.F., Moon, A.M., Illingworth, E.A., Basson, M.A., Scambler, P.J. Tbx1 controls cardiac neural crest cell migration during arch artery development by regulating Gbx2 expression in the pharyngeal ectoderm. *Development* **136**, 3173-3183 (2009).

89 Greulich, F., Rudat, C., Kispert, A. Mechanisms of T-box gene function in the developing heart. *Cardiovasc Res.* **91**, 212-222 (2011).

90 Digilio, M. C., Angioni, A., De Santis, M., Lombardo, A., Giannotti, A., Dallapiccola, B., Marino, B. Spectrum of clinical variability in familial deletion 22q11.2: from full manifestation to extremely mild clinical anomalies. *Clin. Genet.* **63**, 308-313 (2003).

91 Pierpont, M. E., Basson, C.T., Benson, D.W. Jr, Gelb, B.D., Giglia, T.M., Gokdmuntz, E., McGee, G., Sable, C.A., Srivastava, D., Webb, C.L.; American Heart Association Congenital Cardiac Defects Committee, Council on Cardiovascular Disease in the Young. Genetic basis for congenital heart defects: current knowledge: a scientific statement from the American Heart Association Congenital Cardiac Defects Committee, Council on Cardiovascular Disease in the Young: endorsed by the American Academy of Pediatrics. *Circulation* **115**, 3015-3038 (2007).

92 Yamagishi, H., Ishii, C., Maeda, J., Kojima, Y., Matsuoka, R., Kimura, M., Takao, A., Momma, K., Matsuo, N. Phenotypic discordance in monozygotic twins with 22q11.2 deletion. *Am J Med Genet.* **78**, 319-321 (1998).

93 Goodship, J., Cross, I., Scambler, P., Burn, J. Monozygotic twins with chromosome 22q11 deletion and discordant phenotype. *J Med Genet.* **32**, 746-748 (1995).

94 Stalmans, I., Lambrechts, D., De Smet, F., Jansen, S., Wang, J., Maity, S., Kneer, P., von der Ohe, M., Swillen, A., Maes, C., Gewillig, M., Molin, D.G.M., Hellings, P., Boetel, T., Haardt, M., Compernolle, V., Dewerchin, M., Plaisance, S., Vlietinck, R., Emanuel, B., Gittenberger-De Groot, A.C., Scambler, P., Morrow, B., Driscol, D.A., Moons, L.,

Esguerra, C.V., Carmeliet, G., Behn-Krappa, A., Devriendt, K., Collen, D., Conway, S.J., Carmeliet, P. *VEGF*: A modifier of the del22q11 (DiGeorge) syndrome? *Nat. Med.* **9**, 173-182 (2003).

95 Choi, M., Klingensmith, J. Chordin is a modifier of tbx1 for the craniofacial malformations of 22q11 deletion syndrome phenotypes in mouse. *PLoS Genet.* **5**, e1000395 (2009).

96 Yamagishi, H., Maeda, J., Hu, T., McAnally, J., Conway, S.J., Kume, T., Meyers, E.N., Yamagishi, C., Srivastava, D. Tbx1 is regulated by tissue-specific forkhead proteins through a common Sonic hedgehog-responsive enhancer. *Genes Dev.* **17**, 269-281 (2003).

97 Garg, V., Yamagishi, C., Hu, T., Kathiriya, I.S., Yamagishi, H., Srivastava, D. *Tbx1* , a DiGeorge Syndrome candidate gene, is regulated by Sonic Hedgehog during pharyngeal arch development. *Dev. Biol.* **235**, 62-73 (2001).

98 Niederreither, K., Subbarayan, V., Dolle, P., Chambon, P. Embryonic retinoic acid synthesis is essential for early mouse post-implantation development. *Nat Genet.* **21**, 444-448 (1999).

99 Vermot, J., Niederreither, K., Garnier, J.M., Chambon, P., Dolle, P. Decreased embryonic retinoic acid synthesis results in a DiGeorge syndrome phenotype in newborn mice. *Proc Natl Acad Sci USA.* **100**, 1763-1768 (2003).

100 Roberts, C., Ivins, S.M., James, C.T., Scambler, P.J. Retinoic aciddown-redulates Tbx1 expression in vivo and in vitro. *Dev Dyn* **232**, 928-938 (2005).

101 Ryckebusch, L., Bertrand, N., Mesbah, K., Bajolle, F., Niederreither, K., Kelly, R.G., Zaffran, S. Decreased levels of embryonic acid synthesis accelerate recovery from arterial growth delay in a mouse model of DiGeorge syndrome. *Circ Res* **106**, 686-694 (2010).

102 Lammer, E. J., Chen, D.T., Hoar, R.M., Agnish, N.D., Benke, P.J., Braun, J.T., Curry, C.J., Fernhoff, P.M., Grix, A.W. Jr., Lott, I.T, et al. Retinoic acid embryopathy. *N Engl J Med.* **313**, 837-841 (1985).

103 Ross, S. A., McCaffery, P.J., Drager, U.C., De Luca L.M. Retinoids in embryonal development. *Physiol Rev.* **80**, 1021-1054 (2000).

104 Niederreither, K., Vermot, J., Messaddeq, N., Schuhbaur, B., Chambon, P., Dolle, P. Embryonic retinoic acid synthesis is essential for heart morphogenesis in the mouse. *Development* **128**, 1019-1031 (2001).

105 Gosseye, S., Golaire, M.C., Verellen, G., Van Lierde, M., Claus, D. Association of bilateral renal agenesis and DiGeorge syndrome in an infant of a diabetic mother. *Helv Paediatr Acta.* **37**, 471-474 (1982).

106 Ferencz, C., Rubin, J.D., McCarter, R.J., Clark, E.B. Maternal diabetes and cardiovascular malformations: predominance of double outlet right ventricle and truncus arteriosus. *Teratology* **41**, 319-326 (1990).

107 Wilson, T. A., Blethen, S.L., Vallone, A., Alenick, D.S., Nolan, P., Katz, A., Amorillo, T.P., Goldmuntz, E., Emanuel, B.S., Driscoll, D.A. DiGeorge anomaly with renal agenesis in infants of mothers with diabetes. *Am J Med Genet.* **47**, 1078-1082 (1993).

108 Novak, R. & Robinson, H. Coincident DiGeorge anomaly and renal agenesis and its relation to maternal diabetes. *Am J Med Genet* **50**, 311-312 (1994).

109 Agulnik, S. I., Garvey, N., Hancock, S., Ruvinsky, I., Chapman, D.L., Agulnik, I., Bollag, R., Papaioannou, V., Silver, L.M. Evolution of mouse T-box genes by tandem duplication and cluster dispersion. *Genetics* **144**, 249-254 (1996).

110 Wilson, V., Conlon, F.L. The T-box family. *Genome Biol.* **3** (2002).

111 Sinha, S., Abraham, S., Gronostajski, R.M., Campbell, C.E. Differential DNA binding and transcription modulation by three T-box proteins, T, TBX1 and TBX2. *Gene* **258**, 15-29 (2000).

112 Papaioannou, V. E., Silver, L.M. The T-box gene family. *Bioessays* **20**, 9-19 (1998).
113 Singh, M. K., Christoffels, V.M., Dias, J.M., Trowe, M.O., Petry, M., Schuster-Gossler, K., Buerger, A., Ericson, J., Kispert, A. Tbx20 is essential for cardiac chamber differentiation and repression of Tbx2. *Development* **132**, 2697-2707 (2005).
114 Ribeiro, I., Kawakami, Y., Buescher, D., Raya, A., Rodriguez-Leon, J., Morita, M., Rodriguez-Esteban, C., Izpisua Belmonte, J.C. Tbx2 and Tbx3 regulate the dynamics of cell proliferation during heart remodelling. *PLoS One.* **2** (2007).
115 Packham, E. A., Brook, J.D. T-box genes in human disorders. *Hum. Mol. Genet.* **12**, 37-44 (2003).
116 Naiche, L. A., Harrelson, Z., Kelly, R.G., Papaioannou, V.E. T-box genes in vertebrate development. *Annu Rev Genet.* **39**, 219-239 (2005).
117 van Weerd, J. H., Koshiba-Takeuchi, K., Kwon, C., Takeuchi, J.K. Epigenetic factors and cardiac development. *Cardiovasc Res.* **91**, 203-211 (2011).
118 Wu, J. I., Lessard, J., Crabtree, G.R. Understanding the words of chromatin regulation. *Cell* **136**, 200-206 (2009).
119 Lin, W., Dent, S.Y. Functions of histone-modifying enzymes in development. *Curr Opin Genet Dev* **16**, 137-142 (2006).
120 Varga-Weisz, P. ATP-dependent chromatin remodeling factors: nucleosome shufflers with many missions. *Oncongene* **20**, 3076-3085 (2001).
121 Suzuki, M. M., Bird, A. DNA methylation landscapes:provocative insights from epigenomics. *Nat Rev Genet.* **9**, 465-476 (2008).
122 Bruneau, B. G. Chromatin remodeling in heart development. *Curr Opin Genet Dev* **20**, 505-511 (2010).
123 Miller, S. A., Huang, A.C., Miazgowicz, M.M., Brassil, M.M., Weinmann, A.S. Coordinated but physically separable interaction with H3K27-demethylase and H3K4-methyltransferase activities are required for T-box protein-mediated activation of developmental gene expression. *Genes Dev.* **22**, 2980-2993 (2008).
124 Demay, F., Bilican, B., Rodriguez, M., Carreira, S., Pontecorvi, M., Ling, Y., Goding, C.R. T-box factors: targeting to chromatin and interaction with histone H3 N-terminal tail. *Pigment Cell Res.* **20**, 279-287 (2007).
125 Lewis, M. D., Miller, S.A., Miazgowicz, M.M., Beima, K.M., Weinmann, A.S. T-bet's ability to regulate individual target genes requires the conserved T-box domain to recruit histone methyltransferase activity and a separate family member-specific transactivation domain. *Mol. Cell Biol.* **27**, 8510-8521 (2007).
126 Herron, B. J., Lu, W., Rao, C., Liu, S., Peters, H., Bronson, R.T., Justice, M.J., McDonald, J.D., Beier, D.R. Efficient generation and mapping of recessive developemntal mutations using ENU mutagenesis. *Nat Genet.* **30**, 185-189 (2002).
127 Justice, M. J., Noveroske, J.K., Weber, J.S., Zheng, B., Bradley, A. Mouse ENU mutagenesis. *Hum Mol Genet.* **8**, 1955-1963 (1999).
128 Nolan, P. M., Hugill,A., Cox, R.D. ENU mutagenesis in the mouse: application to human genetic disease. *Brief Funct Genomic Proteomic* **1**, 278-289 (2002).
129 Papathanasiou, P., Goodnow, C.C. Connecting mammalian genome with phenome by ENU mouse mutagenesis: gene combinations specifying the immune system. *Annu Rev Genet.* **39**, 241-262 (2005).
130 Lindsay, E. A. *et al.* Congenital heart disease in mice deficient for the DiGeorge syndrome region. *Nature* **401**, 379-383 (1999).
131 Bentham, J., Michell, A.C., Lockstone, H., Andrew, D., Schneider, J.E., Brown, N.A., Bhattacharya, S. Maternal high-fat diet interacts with embryonic Cited2 genotype to reduce

Pitx2c expression and enhance penetrance of left-right patterning defects. *Hum Mol Genet.* **19**, 339-3401 (2010).

132 Schaefer-Graf, U. M., Buchanan, T.A., Xiang, A., Songster, G., Montoro, M., Kjos, S.L. Patterns of congenital anomalies and relationship to initial maternal fasting glucose levels in pregnancies complicated by type 2 and gestational diabetes. *Am J Obstet Gynecol* **182**, 313-320 (2000).

133 Kochilas, L., Merscher-Gomes, S., Lu, M.M., Potluri, V., Liao, J., Kucherlapati, R., Morrow, B., Epstein, J.A. The role of neural crest during cardiac development in a mouse model of DiGeorge Syndrome. *Dev. Biol.* **251**, 157-166 (2002).

134 Siman, C. M., Gittenberger-De Groot, A.C., Wisse, B., Eriksson, U.J. Malformations in offspring of diabetic rats: Morphometric analysis of neural crest-derived organs and effects of maternal vitamin E treatement. *Teratology* **61**, 355-367 (2000).

135 Cederberg, J., Siman, C.M., Eriksson, U.J. Combined treatement with vitamin E and vitamin C decreases oxidative stress and improves fetal outcome in experimental diabetic pregnancy. *Pediatr Res* **49**, 755-762 (2001).

136 Cederberg, J., Eriksson, U.J. Antioxidative treatement of pregnant diabetic rats diminishes embryonic dysmorphogenesis. *Birth Defects Res A Clin Mol Teratol* **73**, 498-505 (2005).

137 Wu, G., Bazer, F.W., Cudd, T.A., Meininger, C.J., Spencer, T.E. Maternal nutrition and fetal development. *J Nutr.* **134**, 2169-2172 (2004).

138 Nybakken, K., Perrimon, N. Hedgehog signal transduction: recent findings. *Curr Opin Genet Dev* **12**, 503-511 (2002).

139 Roux, C., Wolf, C., Mulliez, N., Gaoua, W., Cormier, V., Chevy, F., Citadelle, D. Role of cholesterol in embryonic development. *Am J Clin Nutr* **71**, 1270S-1279S (2000).

140 Cunniff, C., Kratz, L.E., Moser, A., Natowicz, M.R., Kelley, R.I. Clinical and biochemical spectrum of patients with RSH/Smith-Lemli-Opitz syndrome and abnormal cholesterole metabolism. *Am J Med Genet.* **68**, 263-269 (1997).

141 Smith, A. C., Gropman, A.L., Bailey-Wilson, J.E., Goker-Alpan, O., Elsea, S.H., Blancato, J., Lupski, J.R., Potocki, L. Hypercholesterolemia in children with Smith-Magenis syndrome: del(17) (p11.2p11.2). *Genet Med* **4**, 118-125 (2002).

142 Barker, D. J., Gluckman, P.D., Godfrey, K.M., Harding, J.E., Owens, J.A., Robinson, J.S. Fetal nutrition and cardiovascular disease in adult life. *Lancet* **341**, 938-941 (1993).

143 Godfrey, K. M., Barker, D.J. Fetal nutrition and adult disease. *Am. J. Clin. Nutr.* **71**, 1344S-1352S (2000).

144 Metcalfe, N. B., Monaghan, P. Compensation for a bad start: grow now, pay later? *Trends Ecol. Evol.* **16**, 254-260 (2001).

145 Painter, R. C., Roseboom, T.J., Bleker, O.P. Prenatal exposure to the Dutch famine and disease in later life: an overview. *Reprod. Toxicol.* **20**, 345-352 (2005).

146 Roseboom, T. J., van der Meulen, J.H., Osmond, C., Barker, D.J., Ravelli, A.C., Schroeder-Tanka, J.M., van Montfrans, G.A., Michels, R.P., Bleker, O.P. Coronary heart disease after prenatal exposure to the Dutch famine, 1944-1945. *Heart* **84**, 595-598 (2000).

147 Gong, W., Gottlieb, S., Collins, J., Blescia, A., Dietz, H., Goldmuntz, E., McDonald-McGinn, D.M., Zackai, E.H., Emanuel, B.S., Driscoll, D.A., Budarf, M.L. Mutation analysis of TBX1 in non-deleted patients with features of DGS/VCFS or isolated cardiovascular defects. *J Med Genet.* **38**, E45 (2001).

148 Stoller, J. Z., Epstein, J.A. Identification of a novel nuclear localization signal in Tbx1 that is deleted in DiGeorge syndrome patients harboring the 1223delC mutation. *Hum Mol Genet.* **14**, 885-892 (2005).

149 Pu, W. T., Ishiwata, T., Juraszek, A.L., Ma, Q., Izumo, S. GATA4 is a dosage-sensitive regulator of cardiac morphogenesis. *Dev Biol.* **275**, 235-244 (2004).
150 Schneider, J. E., Boese, J., Bamforth, S.D., Gruber, A.D., Broadbent, C., Clarke, K., Neubauer, S., Lengeling, A., Bhattacharya, S. Identification of cardiac malformations in mice lacking Ptdsr using a novel high-throughput magnetic resonance imaging technique. *BMC Dev Biol* **4** (2004).
151 Nowotschin, S., Liao, J., Gage, P.J., Epstein, J.A., Campione, M., Morrow, B.E. Tbx1 affects asymmetric cardiac morphogenesis by regulating Pitx2 in the secondary heart field. *Development* **133**, 1565-1573 (2006).
152 Bose, J., Gruber, A.D., Helming, L., Schiebe, S., Wegener, I., Hafner, M., Beales, M., Kontgen, F., Lengeling, A. The phosphatidylserine receptor has essential functions during embryogenesis but not in apoptotic cell removal. *J Biol* **3** (2004).
153 Curators, M. G. I. S. Human to Mouse ISO GO annotation transfer. (2010).
154 Webby, C. J., Wolf, A., Gromak, N., Dreger, M., Kramer, H., Kessler, B., Nielsen, M.L., Schmitz, C., Butler, D.S., Yates, J.R. 3rd, Delahunty, C.M., Hahn, P., Lengeling, A., Mann, M., Proudfoot, N.J., Schofield, C.J., Bottger, A. Jmjd6 catalyses lysyl-hydroxylation of U2AF65, a protein associated with RNA splicing. *Science* **325**, 90-93 (2009).
155 Chang, B., Chen, Y., Zhao, Y., Bruick, R.K. JMJD6 is a histone arginine demethylase. *Science* **318**, 444-447 (2007).
156 El Omari, K., De Mesmaeker, J., Karia, D., Ginn, H., Bhattacharya, S., Mancini, E.J. Structure of the DNA-bound T-box domain of human TBX1, a transcription factor associated with DiGeorge syndrome. *Proteins* **10.1002/prot.23208** (2011).